대한영상의학회지

CT Findings of Central Airway Lesions Causing Airway Stenosis-Visualization and Quantification: A Pictorial Essay

협착을 유발하는 중심 기관지 병변들의 전산화단층촬영 소견-시각화 및 정량화: 임상화보

Myeong Jin Choi, MD ⓘD, Hee Kang, MD* ⓘD

Department of Radiology, Kosin University Gospel Hospital, Kosin University College of Medicine, Busan, Korea

ORCID iDs
Myeong Jin Choi ⓘD
https://
orcid.org/0000-0002-4552-6810
Hee Kang ⓘD
https://
orcid.org/0000-0001-8065-5477

The tracheobronchial tree is a system of airways that allows the passage of air to aerate the lungs and entire body. Several pathological conditions can affect this anatomical region. Multidetector CT (MDCT) helps identify and characterize various large airway diseases. Post-processing tools, such as virtual bronchoscopy and automatic lung analysis, can help enhance the performance of imaging studies. In this pictorial essay review, we provide imaging findings of various bronchial lesions manifested as wall thickening and endoluminal nodules on conventional MDCT and advanced image visualization and analysis.

Index terms Bronchi; Constriction; Multidetector Computed Tomography; Bronchoscopy

INTRODUCTION

The trachea and the main, lobar, and segmental bronchi are considered to be the "large airways," and a wide spectrum of diseases can occur in this anatomic region (1). Pathologic conditions affecting the central airways include benign and malignant neoplasms, and non-neoplastic conditions (2). Tumors in the tracheobronchial tree are rare, accounting for less than 0.4% of all body tumors. The vast majority of tracheobronchial tumors in adults are known to be malignant (3). In the early stages, both benign and malignant endobronchial tumors may have similar signs and symptoms, which can be misdiagnosed as asthma, chronic obstructive pulmonary disease (COPD), or pulmonary infection (4). Non-neoplastic diseases of the central airways may be in-

fectious, postinfectious, posttraumatic, inflammatory, or idiopathic. CT enables both the detection and characterization of central airway disease (5), and the ability of radiologists to identify lesions in the large airways has been improved to a substantial degree by the routine use of volumetric multidetector CT (MDCT) (1). The performance of the imaging study can be enhanced by post-processing tools such as virtual bronchoscopy (VB) (2). In this pictorial essay review, we will provide guidance in the diagnostic approach for various bronchial lesions manifesting as wall thickening and endoluminal nodules in conventional MDCT images and advanced image visualization and analysis.

ANATOMY OF THE AIRWAY

The trachea is the longest segment of the upper airway, extending from the cricoid cartilage (6th cervical vertebral level) to the carina (5th thoracic vertebral level). The trachea measures about 10–16 cm in length until the branch point of the main carina is reached. The coronal diameter of the normal trachea ranges from 13 to 25 mm in male and 10 to 21 mm in female, and the sagittal diameter ranges from 13 to 27 mm in male and 10 to 23 mm in female. The normal tracheal wall is 1–3 mm thick. The trachea consists of 4 layers, including an inner mucosal layer, a submucosal layer, cartilage and muscle (specifically the trachealis muscle), and an outer adventitial layer, which includes lymphatic and connective tissue. Anteriorly and laterally, the trachea is supported by 16–22 C-shaped cartilaginous rings that protect the integrity of the airway during expiration. The posterior tracheal wall, also known as the membranous portion of the trachea, lacks cartilaginous support and is formed primarily by the thin trachealis muscle (6-9).

The trachea divides at the level of the sternal angle (4th to 5th vertebral levels) at the carina into the right and left mainstem bronchi that extend inferolaterally into the pulmonary hila. The right mainstem bronchus is shorter, has a more vertical course, and originates more superiorly than the left mainstem bronchus. The mainstem bronchi divide into lobar bronchi; 3 on the right side and 2 on the left side. The lobar bronchi further divide into segmental and subsegmental bronchi (Fig. 1, Table 1). Approximately 23 generations of branching occur until the bronchi form the alveoli (Fig. 2) (6, 7). The secondary pulmonary lobule refers to the smallest lung unit measuring from 1 to 2.5 cm in diameter. It is marginated by the interlobular septa containing pulmonary veins and lymphatics, and each secondary lobule is supplied by a small bronchiole and a pulmonary artery branch. Secondary pulmonary lobules are usually composed of acini. The pulmonary acinus is the portion of the lung distal to a terminal bronchiole that is smaller than the secondary pulmonary lobule. It is the last purely conducting airway and is supplied by a first-order respiratory bronchiole or bronchioles. An acinus is the largest lung unit where all airways participate in gas exchange because respiratory bronchioles are the largest airways that have alveoli in their walls (10).

IMAGING TECHNIQUE AND CLINICAL IMPLICATIONS

CT is the primary imaging tool used to evaluate the trachea and central airways. MDCT provides high-resolution images that can be used to generate multiplanar reformations, min-
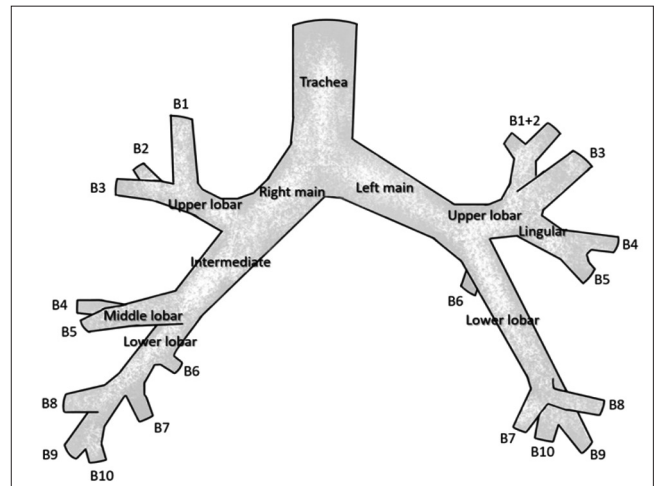
Fig. 1. Lobar and segmental bronchial anatomy.

Table 1. Lung Segments and Segmental Bronchus

	Right Lung		Left Lung
B1	Apical	B1 + B2	Apicoposterior
B2	Posterior		
B3	Anterior	B3	Anterior
B4	Lateral	B4	Superior lingular
B5	Medial	B5	Inferior lingular
B6	Superior	B6	Superior
B7	Medial basal	B7 + B8	Anteromedial basal
B8	Anterior basal		
B9	Lateral basal	B9	Lateral basal
B10	Posterior basal	B10	Posterior basal

Fig. 2. Divisions of the bronchial tree.
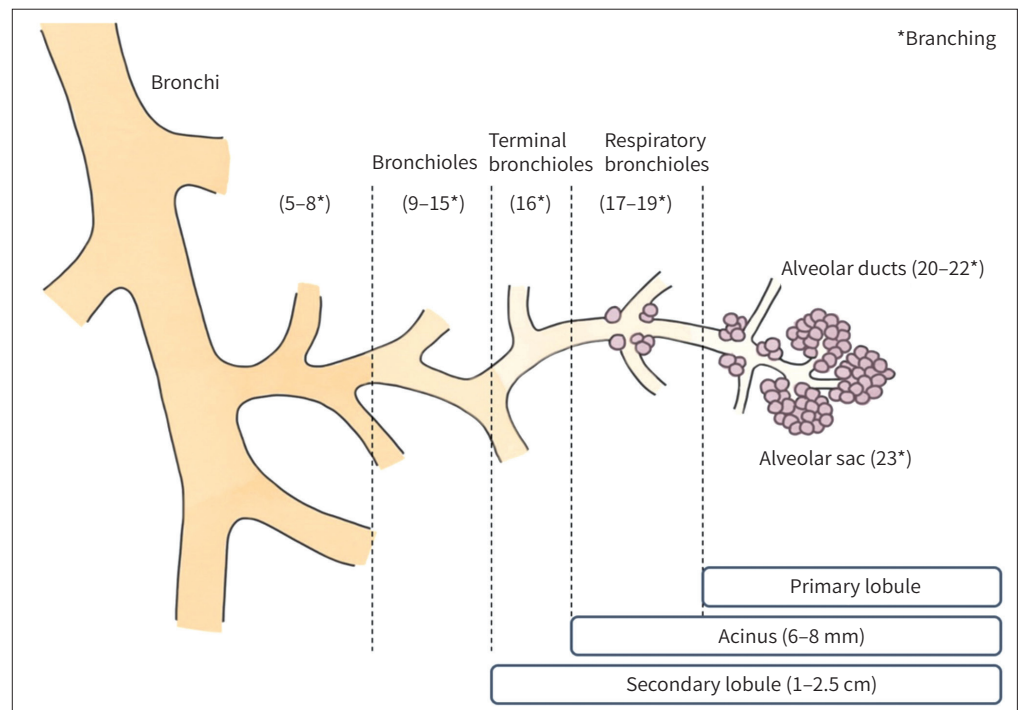
imum intensity projections, and three-dimensional (3D) volume-rendered images for VB (6, 8). VB is a CT-based imaging technique that allows a noninvasive intraluminal evaluation of the tracheobronchial tree (Fig. 3). Several studies have shown that VB can accurately visual-

Fig. 3. Airway analysis of a 62-year-old female who underwent radiation therapy for tracheal squamous cell carcinoma.
A. Contrast-enhanced axial CT shows mild circumferential wall thickening of the trachea and right pleural effusion.
B-E. Multiplanar reformation and three-dimensional volume-rendering images for tracheal visualization and quantification.
F, G. Straightening and short axial images for quantification of tracheal wall thickness at the level of arrows in (B-E). WT: 1.42 mm, WT%: 15%, LA: 208.3 mm^2, WA: 79 mm^2, WA%: 28%, D$_{in}$: 13.2/17.7, D$_{out}$: 16.2/20.4.
D$_{in}$ = minimum inner diameter/maximum inner diameter, D$_{out}$ = minimum outer diameter/maximum outer diameter, LA = plane area of the airway, WA = wall area, WA% = (WA[WA+LA]) × 100, WT = wall thickness, WT% = (WT/[mean diameter/2]) × 100
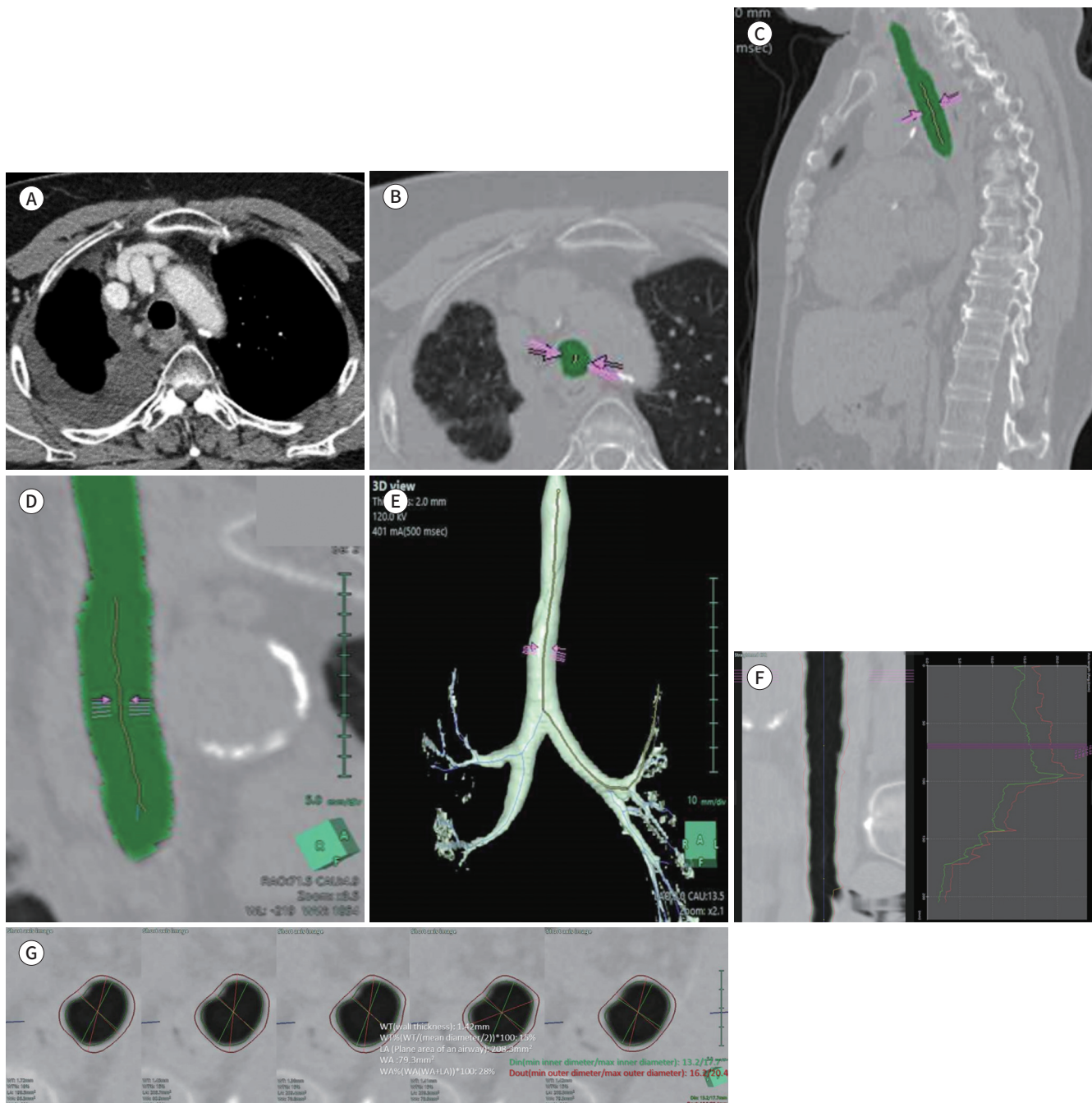
ize the lumen and the diameter of the trachea, the left and right mainstem bronchi, and the bronchial tree down to the fourth-order of bronchial orifices and branches. Accurate evaluation of the morphology of the carina is also possible, and the images are found to be very similar to that of fiberoptic bronchoscopy (FB). Although it is not used on a daily basis, VB can be used in a number of clinical settings. VB is less invasive than FB and therefore, can be used in very young children in whom the use of FB is restricted due to its invasive nature and the need for general anesthesia. When used with axial CT images and coronal or sagittal reconstructions, VB can also help determine the best location for a transbronchial biopsy. This is particularly applicable to the lesions that do not affect the mucosa or distort the airways (Fig. 4, Supplementary Video 1 in the online-only Data Supplement). This can help the bronchoscopist to determine the optimum pathway for passing instruments beyond the field of view. VB can help guide endobronchial procedures (e.g., laser photocoagulation, brachytherapy, endobronchial cryotherapy, endobronchial stent placement, etc.). It can also help with postoperative assessment following the treatment of the bronchial tree, and the evaluation of surgical sutures after lung transplantation, lobectomy, and pneumectomy is also possible (11).

PRIMARY MALIGNANT NEOPLASMS

Primary malignant tumors in the tracheobronchial tree are uncommon, accounting for less than 1% of all thoracic malignancies. Approximately two-thirds of primary malignant tumors are carcinomas originating from the surface epithelium (most commonly squamous cell carcinoma; SCC) or the salivary glands (most commonly adenoid cystic carcinoma; ACC). Other primary tracheobronchial malignancies such as mucoepidermoid carcinoma (MEC), carcinoid tumor, lymphoma, plasmacytoma, sarcoma, and adenocarcinoma are very rare. Primary malignant tumors can produce symptoms of airway obstruction (dyspnea, wheezing, stridor), mucosal irritation and ulceration (cough, hemoptysis), or direct invasion and involvement of adjacent structures (recurrent laryngeal nerve palsy, dysphagia) (3).

SQUAMOUS CELL CARCINOMA

SCC is the most common tracheobronchial malignancy, comprising approximately one-

Fig. 4. An 82-year-old male confirmed with lung adenocarcinoma.
A-C. Axial CT in the lung window setting and three-dimensional volume-rendering image for pathway tracing.
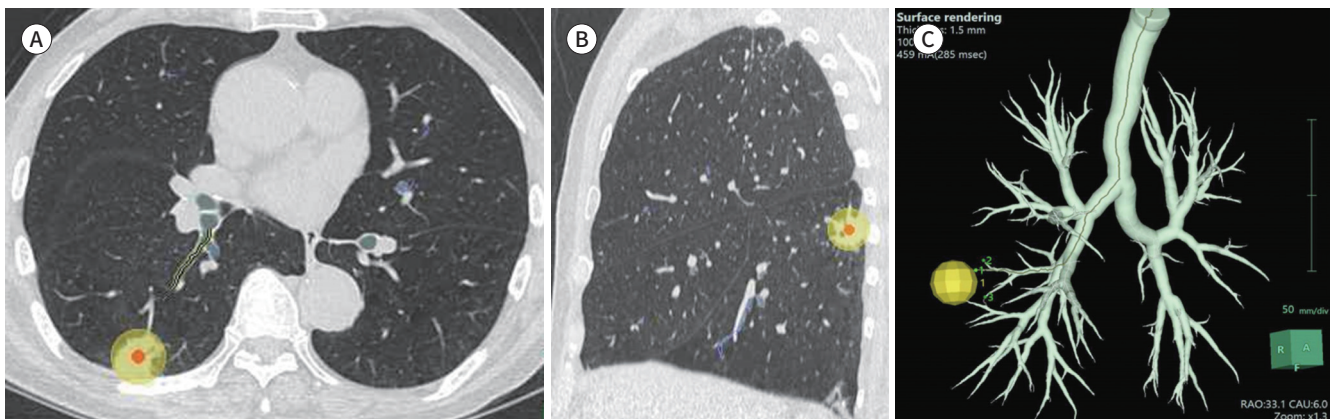
third. SCC has a strong association with habitual cigarette smoking and occurs more commonly in male in their sixth to seventh decades. SCC can be exophytic or infiltrative and tends to involve the posterior wall of the lower two-thirds of the trachea but can occur anywhere in the central airway. About one-third of patients have either mediastinal or pulmonary metastases at diagnosis. In addition, approximately 40% of tracheobronchial SCCs are reported to have an association with carcinoma of the oropharynx, larynx, and lung (3, 9, 12).

On CT, the tumor may appear as a polypoid lesion, a focal sessile lesion, eccentric narrowing of the airway lumen, or circumferential wall thickening. The tumor surface is typically irregular since SCC arises from the surface epithelium (Fig. 5). The majority of SCCs in the tracheobronchial tree show high uptake of fluorine-18-fluorodeoxyglucose (^{18}F-FDG) in PET/CT. Approximately 10% of lesions are multifocal, which necessitates a careful evaluation of the remainder of the airway when SCC is suspected (3, 9, 12).

ADENOID CYSTIC CARCINOMA

ACC is one of the more common tracheal neoplasms of salivary gland origin with a similar prevalence to that of SCC, comprising approximately one-third of all primary tracheal neo-

Fig. 5. A 77-year-old male with squamous cell carcinoma complaining of cough and blood-tinged sputum.
**A, B.** Contrast-enhanced chest CT shows an endobronchial enhancing mass with branching appearance in the right lower lobe.
C. CT shows avid FDG uptake on ^{18}F-FDG PET/CT (maximum standardized uptake value: 18.5).
D. The three-dimensional volume-rendering image shows smooth tapering of the right intermediate bronchus. The pulmonary function test showed a moderate obstructive lung defect with a forced expiratory volume in 1 second of 61%.
E. Bronchoscopic biopsy confirmed the endobronchial tumor to be squamous cell carcinoma with papillary architecture.
^{18}F-FDG = fluorine-18-fluorodeoxyglucose
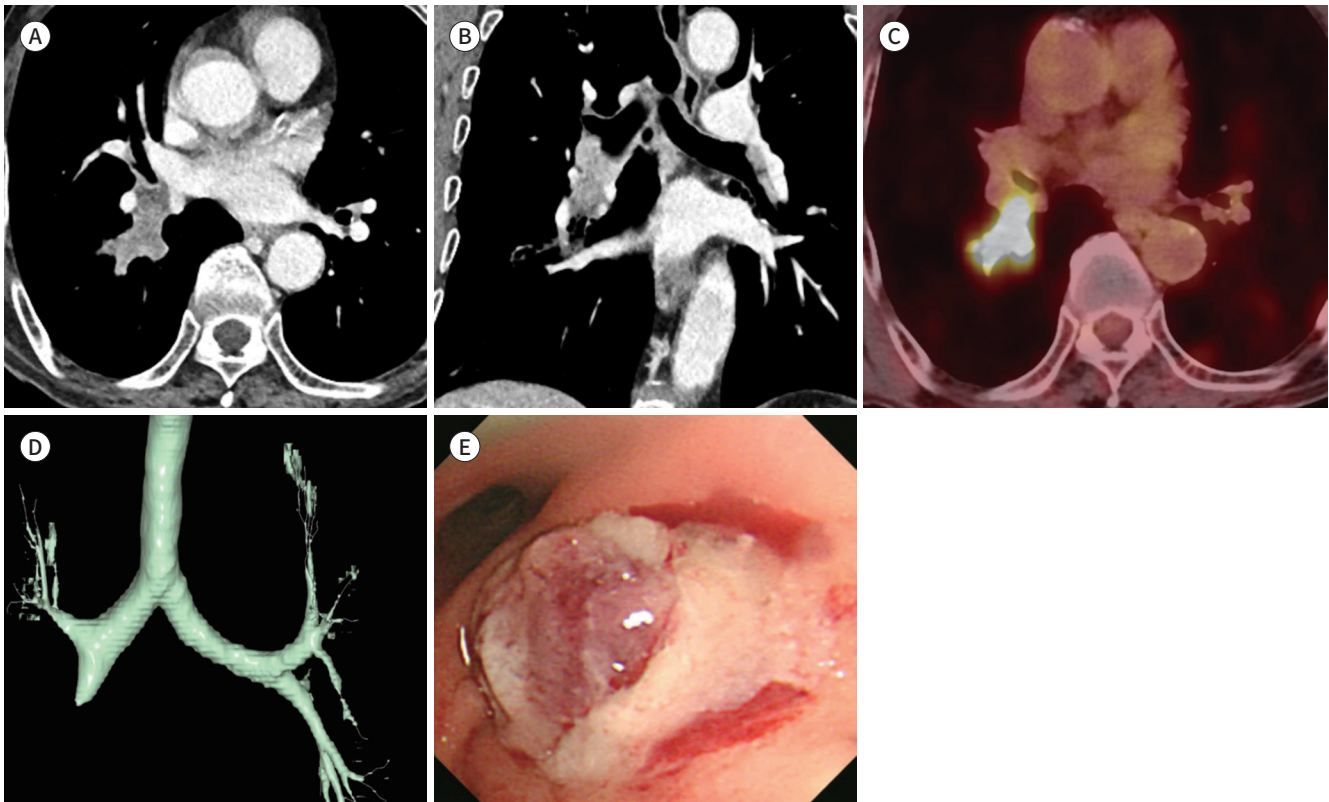
plasms. ACC has an equal sex distribution, occurs most often in the fifth decade, and is not associated with cigarette smoking. ACC tends to occur in the central airways such as the trachea, main bronchus, or lobar bronchus; a peripheral or segmental location is uncommon. Because of its submucosal origin, ACC tends to have an intact epithelium and a smooth contour. Pathologically, these tumors resemble glandular tissue, as they arise from minor salivary glands (3, 9, 12).

The typical CT finding is a soft tissue mass, commonly located in the proximal half of the trachea, and more frequently along the posterolateral wall (Fig. 6). The tumor typically demonstrates an extensive submucosal and transmural spread and manifests with circumferential and infiltrative growth. Metastases are very unusual, with recurrence more often being

Fig. 6. A 60-year-old male confirmed with adenoid cystic carcinoma without respiratory symptoms.
A, B. Contrast-enhanced chest CT shows eccentric focal wall thickening with mild enhancement in the trachea (arrows).
C. The three-dimensional volume-rendering image shows smooth asymmetric luminal narrowing (arrow) in the mid-portion of the trachea.
D. Avid FDG uptake (arrow) on ^{18}F-FDG PET/CT (maximum standardized uptake value: 3.8).
E. Bronchoscopic biopsy confirmed the focal protruding lesion to be adenoid cystic carcinoma.
^{18}F-FDG = fluorine-18-fluorodeoxyglucose
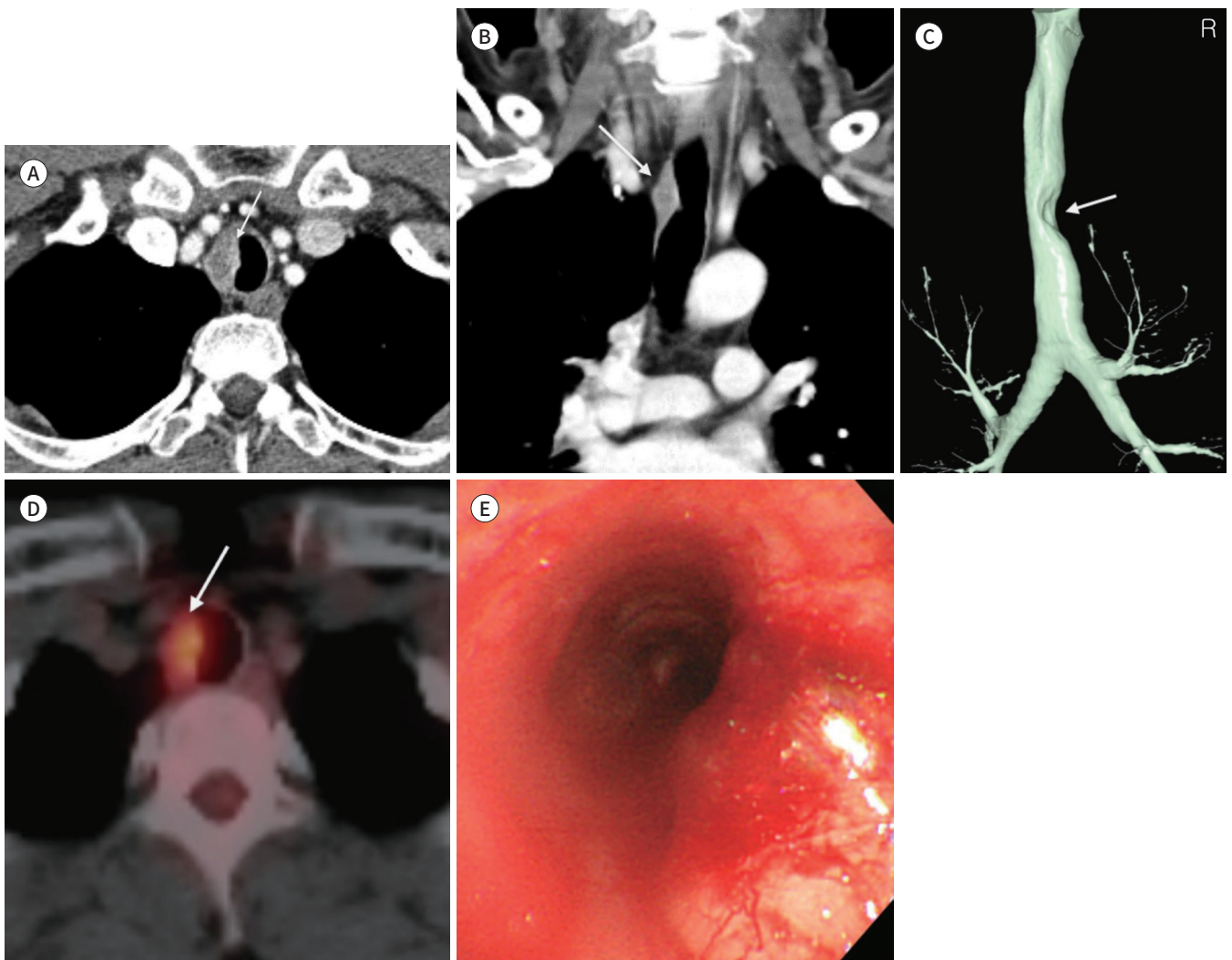
local. It can demonstrate high FDG uptake in ^{18}F-FDG PET/CT imaging depending on the grade of the tumor; avid and homogeneous FDG uptake is found in the high- and intermediate-grade tumors rather than the low-grade tumors. The cephalocaudal extent of the tumor may be underestimated at CT, therefore evaluation with 3D or multiplanar reconstruction is required. Since most ACCs manifest as central airway tumors, they should be distinguished from bronchogenic carcinoma (e.g., SCC), carcinoid tumor, and benign airway tumors. When ACCs occur in the central airways and show avid FDG uptake it is difficult to differentiate them from bronchogenic carcinoma, particularly SCC (3, 9, 12).

MUCOEPIDERMOID CARCINOMA

MEC in the tracheobronchial tree is rare, accounting for only 0.1%–0.2% of all pulmonary malignancies. Similar to ACC and pleomorphic adenoma, MEC arises from minor salivary gland tissue, most often in the central airways. MEC occurs in patients from 4 to 78 years of age, and nearly one-half of the patients are under 30 years old. Clinical presentation is variable, ranging from asymptomatic to coughing, wheezing, and/or hemoptysis, usually in young patients. Most MECs occur in the lobar or segmental bronchi rather than the trachea or main bronchi (3, 9).

The appearance of MEC in CT is quite variable. The tumor often appears as an enhancing intraluminal nodule with smooth or lobulated contours, with or without punctate internal calcifications (Fig. 7). Cavitary lesions, as well as diffuse tracheal wall thickening, have also been described (9). Obstructive pneumonia, atelectasis, and mucus plugging are frequently associated findings, particularly when the tumor is located in the segmental bronchi. MECs have been reported to show variable amounts and patterns of FDG uptake. High and homogeneous FDG uptake has been reported in high-grade MECs, whereas mild FDG uptake is found in low-grade MECs. As with ACCs, MECs in the central airways with high FDG uptake may be difficult to differentiate from bronchogenic carcinoma, especially SCC (3, 9).

CARCINOID TUMOR

Carcinoid tumors originate from neuroendocrine (Kulchitsky) cells and comprise less than 2% of all tracheobronchial primary malignant neoplasms. Carcinoid tumors in the tracheobronchial tree usually involve the main, lobar, or segmental bronchi. Carcinoid tumors usually do not have any association with cigarette smoking. Patients are usually in their third to fifth decade, and commonly present with symptoms related to airway involvement, such as asthma, cough, dyspnea, and hemoptysis. As the majority of tumors arise in or close to the central airways, airway obstruction can occur resulting in atelectasis or recurrent postobstructive pneumonia in the same lobe (3, 9, 12).

There are two histologic subtypes of bronchial carcinoid. Typical carcinoids comprise up to 90% of bronchial carcinoids. They are generally small, do not metastasize to regional lymph nodes, and are associated with an excellent prognosis, with surgical resection resulting in a cure in the majority of cases. These tumors are classically slow growing with a doubling time usually greater than 2 years. Atypical carcinoids are generally larger, metastasize to regional lymph nodes, and are associated with a worse prognosis (3, 9, 12).

On CT, a carcinoid tumor in the tracheobronchial tree appears as a well-defined spheric or

Fig. 7. A 59-year-old male with mucoepidermoid carcinoma complaining for 2 months of dyspnea on exertion.
A, B. Contrast-enhanced chest CT shows a well-defined central enhancing nodule (arrows) in the left main bronchus and endobronchial secretion in the distal portion (arrowheads).
C. 18F-FDG PET/CT shows a focal hypermetabolic lesion (arrow) in the left main bronchus (maximum standardized uptake value: 3.4).
D. Bronchoscopy shows a necrotic polypoid mass in the left main bronchus. The endobronchial mass was confirmed to be low-grade mucoepidermoid carcinoma during surgery for bronchial resection.
18F-FDG = fluorine-18-fluorodeoxyglucose
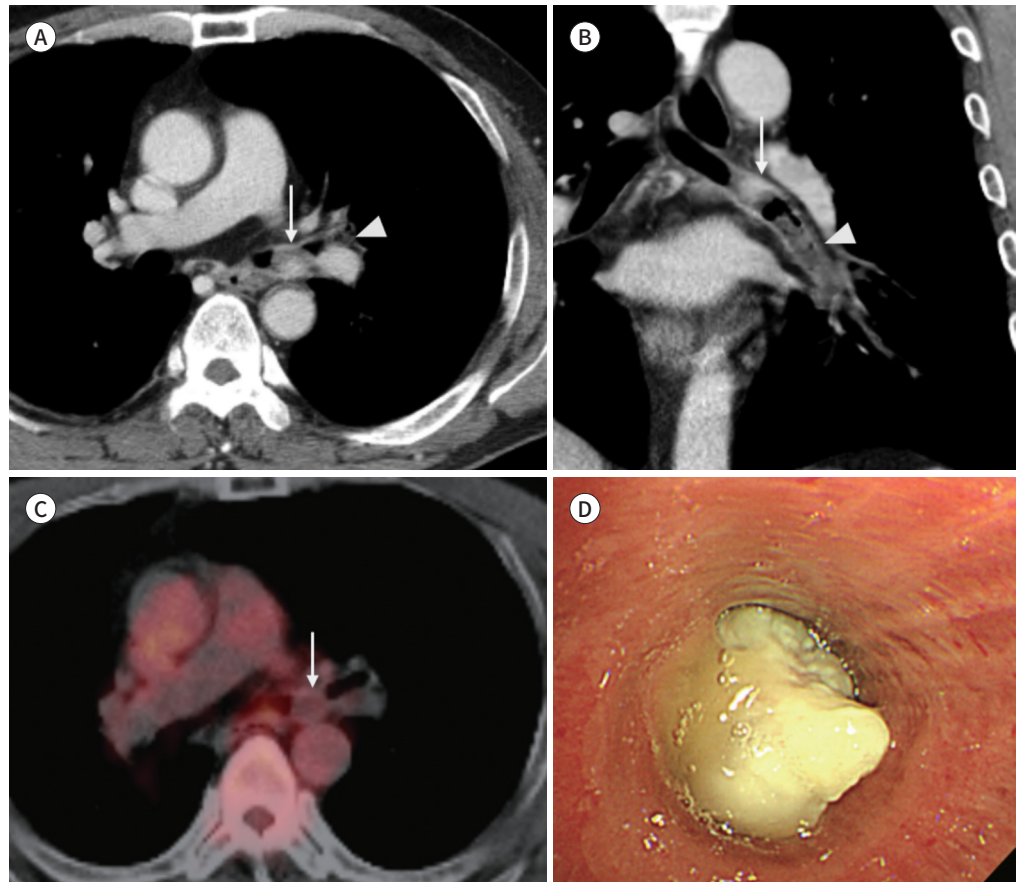
ovoid nodule of homogeneous soft-tissue attenuation with a slightly lobulated border (Fig. 8). The tumor may manifest as a small nodule located entirely within the bronchial lumen; however, the intraluminal component may be relatively small compared with the large extraluminal component giving an appearance that resembles a tip of an iceberg (iceberg tumor). Carcinoid tumors tend to be vascular and may demonstrate intense enhancement, which is particularly helpful in distinguishing the tumor from obstructive atelectasis or an adjacent mucus plug. Internal calcifications may be present in up to one-third of cases. On 18F-FDG PET/CT, carcinoid tumors have been reported to have lower uptake than other malignant tumors, resulting in a high false-negative rate (3, 9, 12).

Fig. 8. A 15-year-old girl with a carcinoid tumor complaining of persistent fever, sweating, and myalgia.
A, B. Contrast-enhanced chest CT shows a well-defined round enhancing nodule in the left main bronchus (arrows).
C. CT in the lung window setting shows peribronchial patchy consolidation and bronchiolitis, suggesting post-obstructive pneumonia in the left lower lobe.
D. Bronchoscopy shows a well-defined polypoid mass with intraluminal obstruction in the left main bronchus. The patient underwent left lower lobectomy and was confirmed with typical carcinoid.
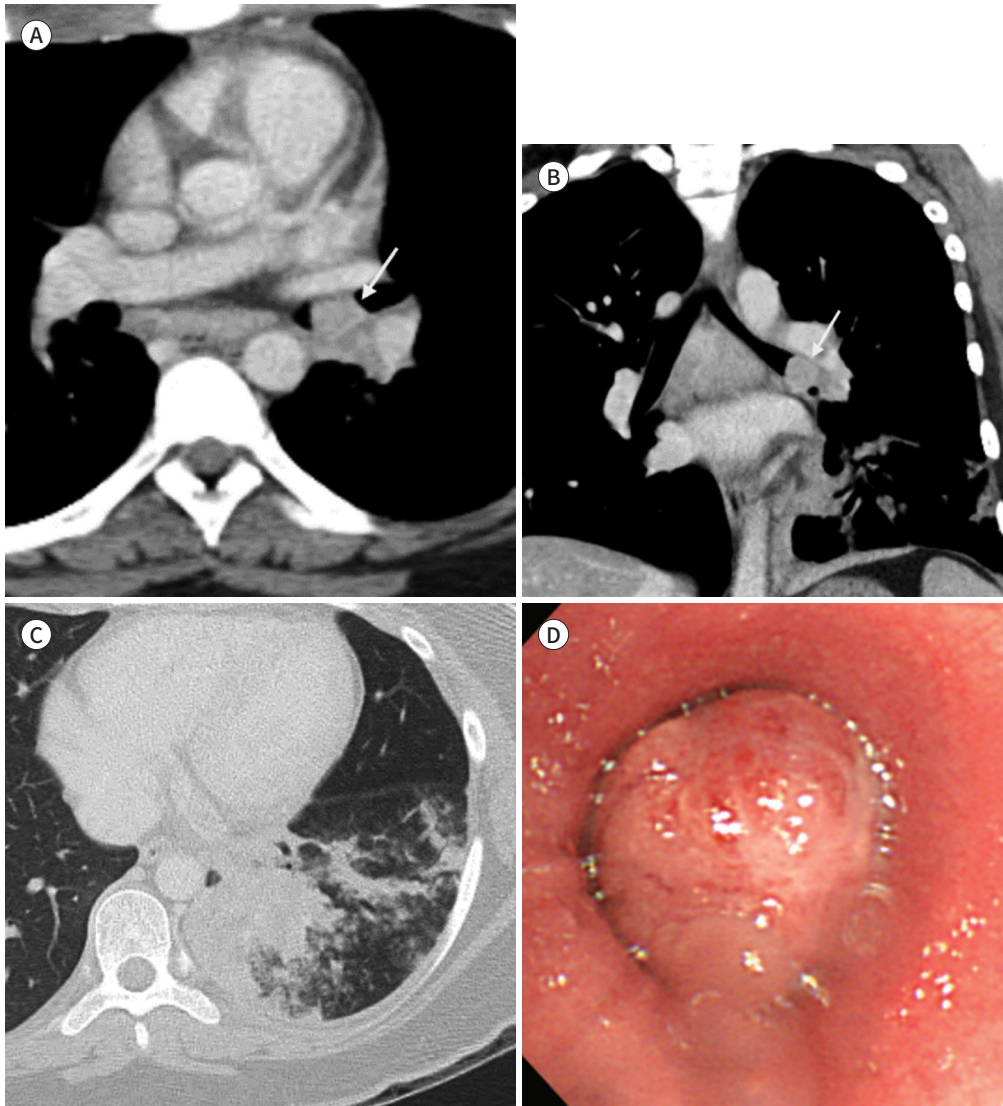
DIRECT INVASION BY OTHER MALIGNANCIES

Secondary malignancies in the tracheobronchial tree may occur as a result of hematogenous spread or direct invasion by a malignancy of the lung, larynx, esophagus, thyroid gland, or mediastinum, with direct invasion being far more common. In cases of direct airway spread from a primary tumor, it is important for diagnosis to establish whether the tumor is centered outside the airway, for example, in the esophagus, lung, or thyroid (4, 12).

The CT imaging is nonspecific as there may be a solitary lesion, multiple lesions, or eccen-

tric wall thickening (3).

ESOPHAGEAL CANCER

Owing to aggressive growth and the lack of serosal anatomic barrier, esophageal carcinoma has the propensity to spread locally through the esophageal wall into surrounding loose connective tissue and organs such as the trachea, bronchi, lung, thyroid gland, aorta, and pericardium. When the tumors invade the trachea, they are classified as T4b tumors and are unresectable (13).

On CT, tracheal or bronchial involvement is considered certain when an intraluminal mass or a thickened wall is present (Fig. 9), or when tumoral extension is seen between the trachea and the aortic arch between the left main bronchus and the descending aorta (14). Tracheo-bronchial invasion is also suggested by displacement or indentation of the tracheal or bronchial wall by the tumor or by the presence of tracheoesophageal fistula, which occurs in

Fig. 9. A 75-year-old male with direct tracheal invasion from esophageal cancer complaining of hoarseness for 5 months and recent onset of blood-tinged sputum.
**A, B.** Contrast-enhanced CT shows a well-defined enhancing mass invading the posterior membranous tracheal portion originating from the right side of the esophagus (arrows).
C. The three-dimensional volume-rendering image of the airway shows a well-defined protruding mass (arrow) from the posterior membranous portion of the upper trachea.
D. The mass shows avid uptake (arrow) on ^{18}F-FDG PET/CT (maximum standardized uptake value: 11).
E. Endoscopy shows a fungating mass with easy friability, which was confirmed to be squamous cell carcinoma originating from the esophagus.
^{18}F-FDG = fluorine-18-fluorodeoxyglucose
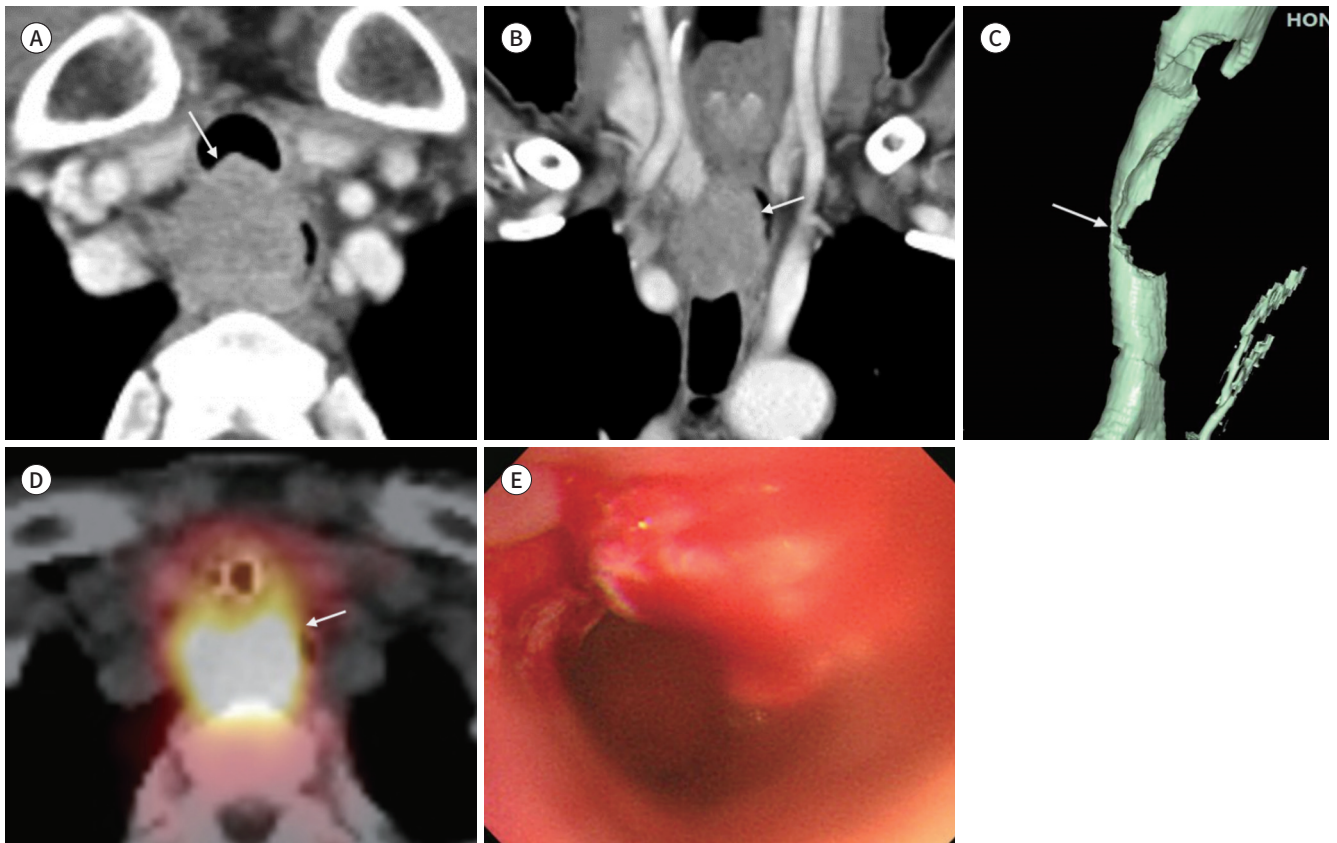
5%–10% of patients particularly in those who have received radiation therapy (12, 13).

THYROID CANCER

Thyroid cancer rarely invades the trachea, but when it does, airway obstruction due to the tracheal invasion by tumors is the direct cause of most deaths (15). The incidence of tracheal invasion is reported to range from 1% to 13% of patients with thyroid carcinoma (16). The worst condition of papillary thyroid carcinoma with tracheal invasion is when the tumor has extended to the endoluminal trachea, with an incidence of 0.5%–1.5% (15).

CT images may demonstrate a mass in the thyroid gland with the mass partially protruding into the lumen, resulting in the thickening of the trachea on the ipsilateral side. The mass may also have obvious enhancement (Fig. 10) (15).

LUNG CANCER

Direct invasion of the trachea by primary lung cancer is often seen and classified as T4 lung cancer according to the American Joint Committee on Cancer lung cancer staging system. In a clinicopathologic study of endotracheal and endobronchial metastases, Kiryu et al. (17) proposed four types of developmental modes of endotracheal and endobronchial metastases morphologically: type 1, direct metastasis to the bronchus; type 2, bronchial invasion by a parenchymal lesion; type 3, bronchial invasion by mediastinal or hilar lymph node metastasis; and type 4, a peripheral lesion extending along the proximal bronchus.

CT images may demonstrate direct invasion and extrinsic compression of the trachea and lymph node (12), which may cause severe lumen stricture and distortion. Invasion and displacement of the tracheobronchial tree may be seen, along with mediastinal lymphadenopathy (18).

METASTASIS

Metastatic involvement of the trachea and large airways is rare and may occur as a result of

Fig. 10. A 78-year-old male with direct tracheal invasion from known follicular thyroid cancer complaining of recurrent asphyxia.
A, B. Contrast-enhanced CT shows an enhancing mass with extracapsular extension in the left thyroid gland (*), mild wall thickening on the left side of the trachea, and right-sided tracheal deviation (arrows).
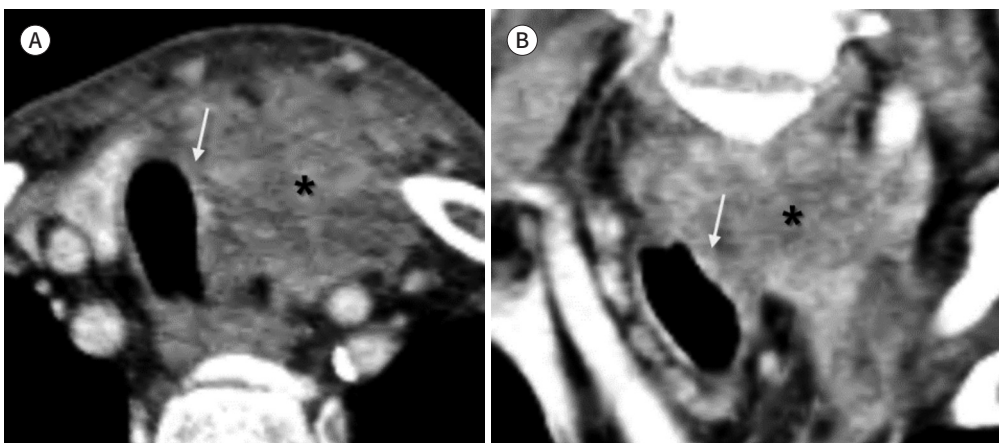
hematogenous spread. The most common primary tumors that spread hematogenously to the large airways are breast, colon, kidney, lung, and melanoma (4).

On CT, these tumors can present as solitary or multiple polypoid nodules with or without the "glove-finger" appearance or as eccentric wall thickening. In rare cases when the metastasis is solitary, it is indistinguishable from a primary airway tumor (i.e., SCC, ACC, or carcinoid). A history of primary adenocarcinoma or melanoma suggests metastatic involvement of the airways. In most cases, the extramural source of an airway tumor is apparent on CT. The degree of FDG uptake depends mostly on the metabolic activity and degree of differentiation of the primary tumor. Since the majority of malignancies have high metabolic activity, ^{18}F-FDG PET/CT usually shows intense uptake (4).

KIDNEY CARCINOMA

Endobronchial metastasis from extrapulmonary malignancy is found in 2%–5% of autopsies performed on patients who died of extrapulmonary malignancy, of which renal cell carcinoma (RCC) is the most common malignancy to involve the bronchus (19). When RCC metastasizes to the large airways, it most often manifests with symptoms similar to a primary endobronchial tumor such as hemoptysis (12).

On CT, the lesions may appear as a strongly enhancing, high attenuation nodule or mass (Fig. 11) (12).

COLORECTAL CARCINOMA

Colorectal carcinomas account for 12%–26% of all endobronchial metastases and are one of the more common causes of central airway involvement by metastatic disease. It is not uncommon for patients to also have pulmonary nodules separate from the endobronchial lesion (20). The endoscopic aspect of the lesion is a bulging or polypoid mass with a necrotic component that bleeds (21).

Whereas 95% of lung metastases are seen on CT scans, only 55% of endobronchial lesions are detected. Imaging findings include nodules, atelectasis, or lymph node enlargement (Fig. 12) (21).

LUNG CANCER

Tracheal metastasis of primary lung cancer is extremely rare. The overall incidence of tracheal metastasis was found to be 0.44% in surgically resected non-small cell lung cancer (0.77% in SCCs and 0.18% in adenocarcinomas), and the incidence of tracheal metastasis was lower in primary lung cancers than in non-pulmonary malignancies (22). Metastases are usually scattered in the lung parenchyma or pleura, and bronchial invasion is sometimes seen as a result of mediastinal or hilar lymph node metastasis. Endobronchial metastases directly involving the bronchial epithelium are rare. Endobronchial metastases from lung cancer usually develop at least several months after the resection of the primary site (23). The symptoms associated with endotracheal and endobronchial metastases regardless of the primary site are similar to those associated with primary endotracheal and endobronchial tumors. Hemoptysis with coughing is the most common symptom, with an incidence of 41%–62% reported (22).

Fig. 11. A 54-year-old male with a history of renal cell carcinoma. He was admitted for radiofrequency abla-tion of bone metastasis.
A, B. Contrast-enhanced CT shows an approximately 1-cm well-defined polypoid-enhancing nodule (ar-rows) in the upper trachea.
C. There was no significant hypermetabolism on ^{18}F-FDG PET/CT because of its undetectable size (arrow).
D. When the patient was intubated for general anesthesia, a small nodule protruded through the endotra-cheal tube. The nodule was confirmed to be metastatic renal cell carcinoma. The patient underwent bron-choscopic cryotherapy for a residual tracheal tumor.
^{18}F-FDG = fluorine-18-fluorodeoxyglucose
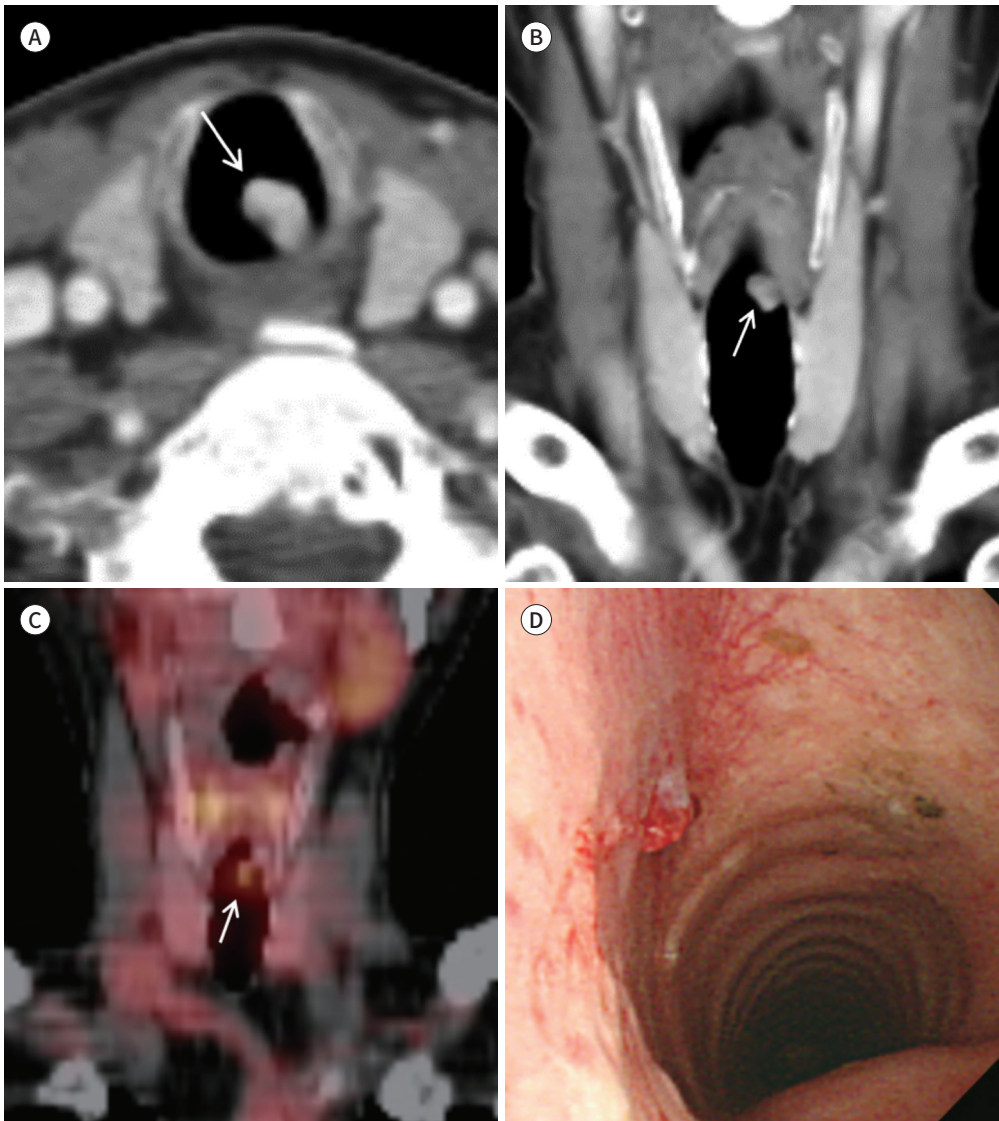
Tracheal metastasis of primary non-small cell lung cancer manifests as an endotracheal nodule or eccentric wall thickening of the trachea, showing significant contrast enhance-ment with a predilection for the upper trachea on CT (Fig. 13) (1, 24).

BENIGN TUMOR

Benign tumors of the tracheobronchial tree are quite rare, accounting for less than 10% of

Fig. 12. A 78-year-old female patient with a history of ascending colon cancer.
A, B. Contrast-enhanced CT shows a focal irregular polypoid nodule (arrows) in the left main bronchus.
C. CT in the lung window setting shows multiple metastatic nodules (arrowheads) in the left lower lobe.
D. ^{18}F-FDG PET/CT shows a localized hypermetabolic lesion (arrow) in the left main bronchus (maximum standardized uptake value: 13.7).
E. Bronchoscopy shows an eccentric endobronchial mass in the left main bronchus with partial obstruction, which was confirmed to be metastatic adenocarcinoma of the colon.
^{18}F-FDG = fluorine-18-fluorodeoxyglucose
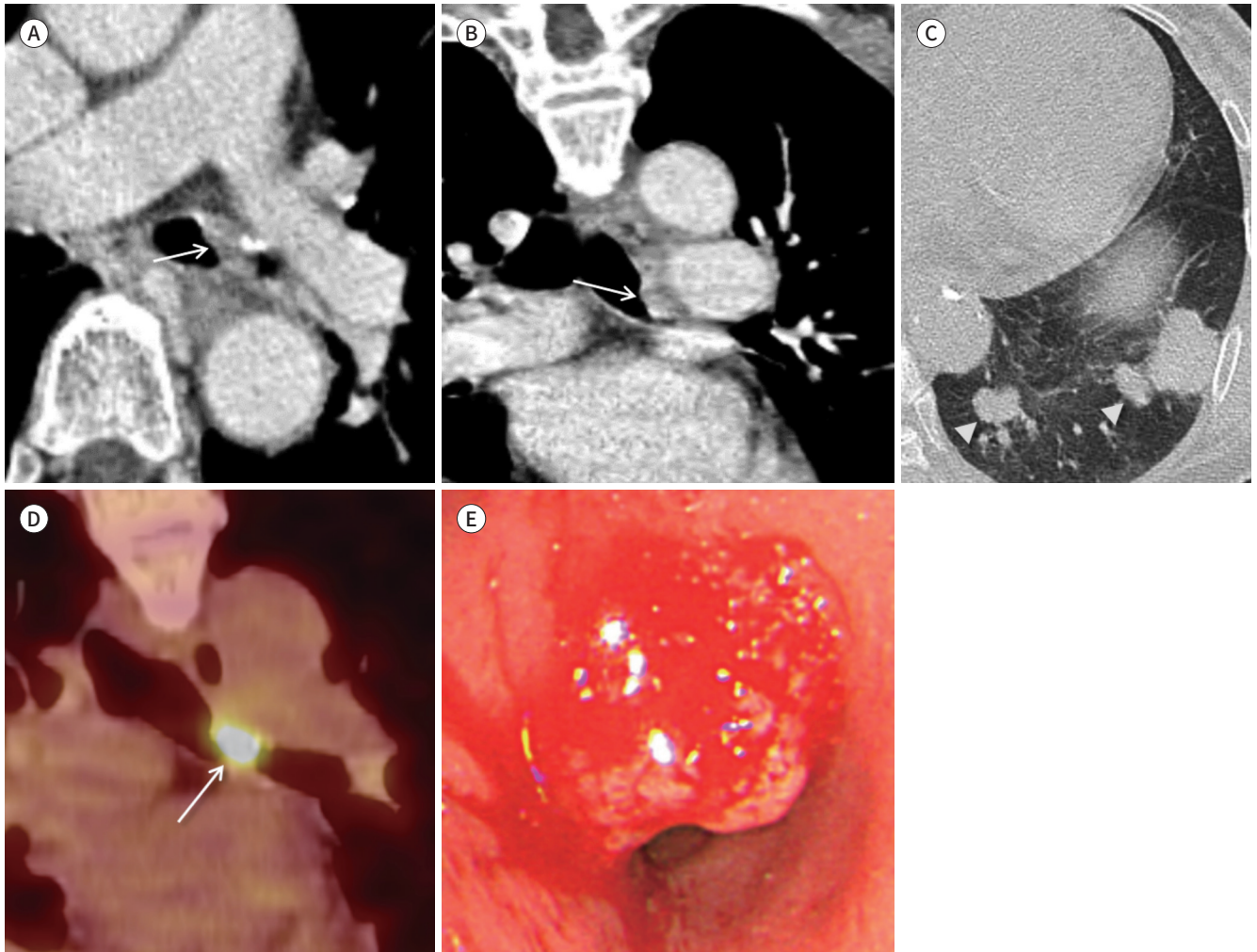
all airway neoplasms. They almost always arise from the mesenchymal tissue. The most common benign tumors are hamartomas and squamous cell papillomas. Other minor tumors such as leiomyoma, neurogenic tumor, lipoma, or mucous gland adenoma may also arise in the tracheobronchial tree. Benign tumors tend to be well-demarcated, round, and less than 2 cm in diameter. Because these tumors originate in the submucosa, the overlying epithelium is usually intact, resulting in a smooth appearance of the tumor surface in the airway lumen. Common symptoms include dyspnea, wheezing, and stridor due to upper airway obstruction. Affected patients, however, tend to be asymptomatic until 50%–75% of the luminal diameter is obstructed. Thus, a benign tumor in the trachea can go unrecognized for months or even years (3).

Fig. 13. A 59-year-old male with a history of right lower lobectomy and chemotherapy for lung squamous cell carcinoma 1 year before.
A, B. Contrast-enhanced CT shows a well-defined enhancing polypoid mass (arrows) on the right posterolateral side of the trachea.
C. ^{18}F-FDG PET/CT shows a localized hypermetabolic lesion (arrow) in the upper trachea (maximum standardized uptake value: 6.1).
D. Preoperative CT shows primary lung cancer with cavitation (*) in the right lower lobe.
E. Bronchoscopy shows a polypoid mass with luminal narrowing in the trachea, which bronchoscopic biopsy confirmed to be metastatic squamous cell carcinoma.
^{18}F-FDG = fluorine-18-fluorodeoxyglucose
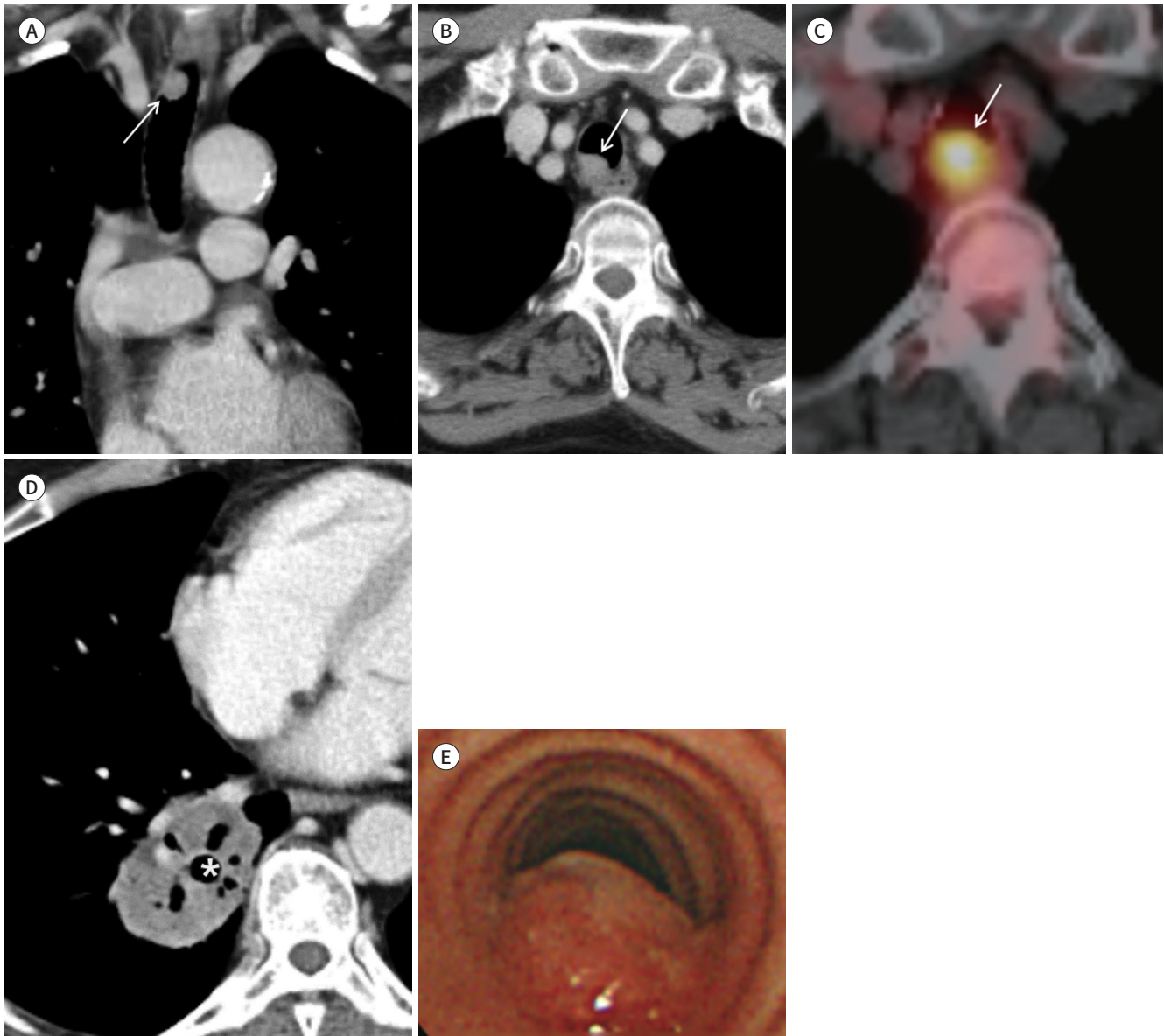
SQUAMOUS CELL PAPILLOMA

Squamous cell papilloma is the most common benign tracheobronchial neoplasm. It represents an abnormal proliferation of the squamous epithelium in the respiratory tract, secondary to infection with the human papilloma virus. When it involves the tracheobronchial tree, this lesion has two forms: multiple and solitary. Most cases correspond to the multiple form of airway papilloma, known as juvenile laryngotracheal papillomatosis. It is a neoplas-

tic growth secondary to infection with human papillomavirus types 6 and 11 in the upper respiratory tract. Solitary papilloma of the tracheobronchial tree is less common and usually occurs in adults. Tracheobronchial compromise is most common in this form and involves just 5% of patients, generally between 20 and 40 years of age, infected by sexual transmission (oral contact), and with a male to female ratio of 4:1. Unlike the multiple form, solitary papil-

Fig. 14. A 42-year-old male with squamous cell papilloma complaining of voice change for 3 months.
A-C. Chest CT in the lung window setting shows multiple polypoid nodules (arrows) along the upper trachea and vocal cord (not shown here).
D. Bronchoscopy shows multiple polypoid nodules along the mucosal surface from the larynx to the mid-trachea, which bronchoscopic biopsy confirmed to be squamous cell papilloma.
This figure has been adapted with permission from Dong-A University Hospital, Busan, South Korea.
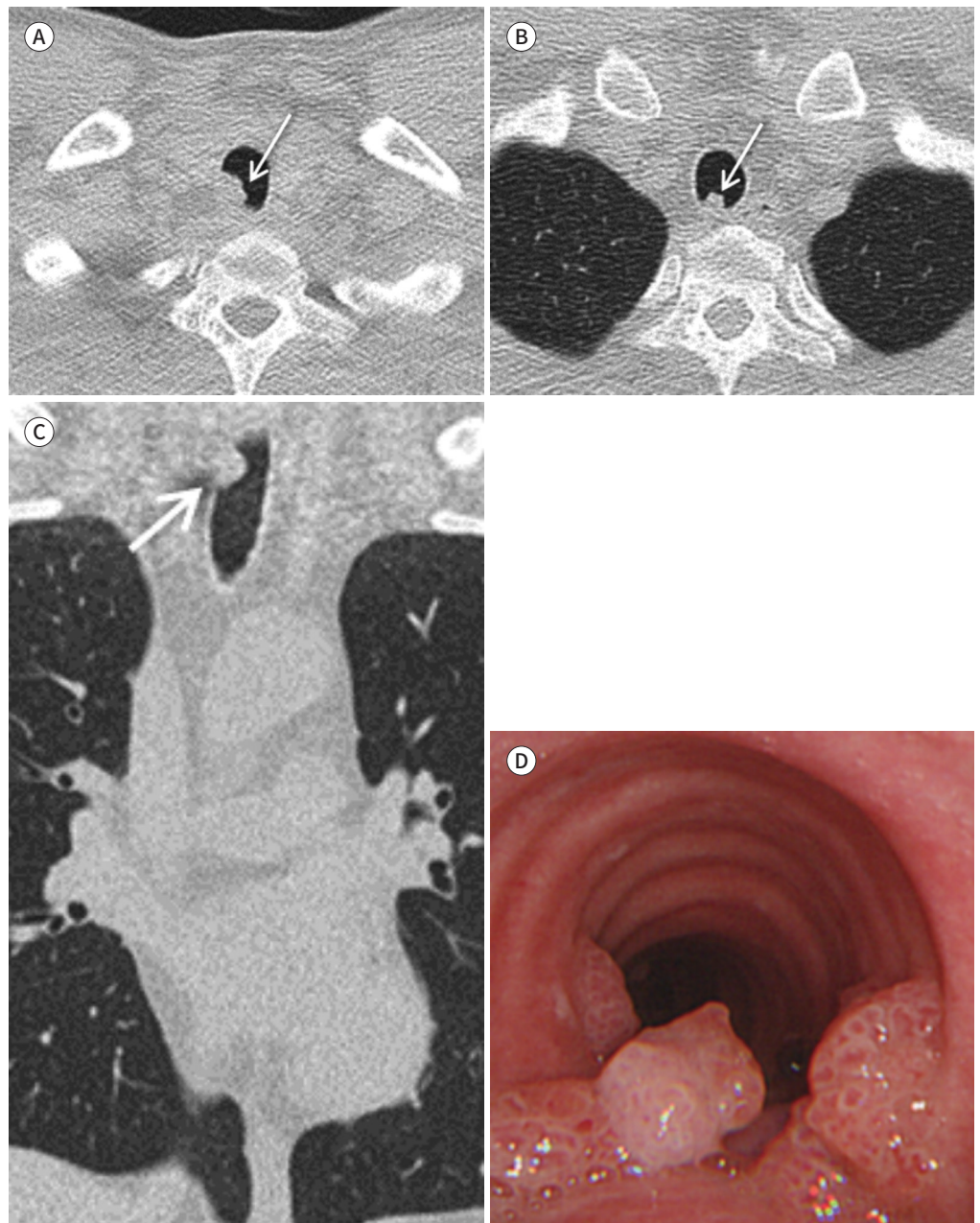
loma is associated with cigarette smoking or arises de novo. Squamous cell papilloma is usually benign in children and may regress. In adults, however, the tumor can infiltrate and become malignant. Gross examination shows papillomas are polypoid or sessile masses within the airways. The lesions are characterized histologically by a proliferation of well-differentiated squamous epithelium with a central fibrovascular core (2, 25).

MDCT shows polypoid nodules arising from the mucosal surface, with intraluminal growth (Fig. 14). Lesions may be single or multiple and may cause atelectasis of the underlying lung, with symptoms of obstructive pneumonia. Pulmonary spread occurs in 1% of patients and manifests on CT as multiple pulmonary nodules with air trapping areas. Involvement of the distal airway can produce pulmonary nodules that frequently have cavitations (2, 25).

HAMARTOMA

Hamartomas are the most common type of benign endobronchial neoplasms with an incidence in general population between 0.025% and 0.32%. These tumors are most commonly located intrapulmonary and endobronchial location (4). It originates from a large bronchus, grows into the lumen, and obstructs the bronchi before becoming large. The most frequent types of endobronchial hamartoma are chondromatous and lipoid. There is also an extremely rare osteochondromatosis variety. Intrapulmonary and endobronchial hamartomas contain cartilage, fat, fibrous tissue, and an epithelial component. It is reported that endobronchial lesions tend to contain relatively more fat than parenchymal lesions, which may be attributable to the relative abundance of fat in the bronchial walls as opposed to the lung parenchyma. Endobronchial hamartoma is often symptomatic because of airway obstruction, which can cause cough, hemoptysis, dyspnea, and obstructive pneumonia. Chest radiography often shows the sequelae of endobronchial obstruction, which include atelectasis, postobstructive pneumonia, and bronchiectasis. Endobronchial mass lesions may be poorly depicted or not depicted at all on chest radiographs (2, 25).

CT scans reflect the various tissue components of hamartoma (Fig. 15). The hamartoma is composed of chondroid cartilage, observed as a popcorn calcification within the lesion, fat, represented by areas of low attenuation, and fibrous and epithelial tissue, both with soft-tissue attenuation. The combination of fat attenuation areas and popcorn calcifications is considered diagnostic for hamartoma on CT. Bronchial hamartomas tend to have more fat than pulmonary hamartomas because the bronchial wall is rich in fat, and popcorn calcification helps to differentiate hamartomas from malignant tumors (2, 25). Bronchoscopic examination shows a polypoid or pedunculated sharply marginated mass with a smooth and yellowish surface without submucosal involvement (4).

INFECTION

Infection of the large airways can be caused by a variety of pathogens. Infections lead to an inflammatory response resulting in nonspecific focal or diffuse wall thickening of the airways, and, occasionally, luminal narrowing (1).

Fig. 15. A 79-year-old male with hamartoma and a history of asthma.
A, B. Contrast-enhanced CT shows a poorly enhancing focal polypoid nodule (arrows) on the right side of the distal trachea.
C. The three-dimensional volume-rendering image of the airway shows a focal round nodule (arrow) with a smooth surface in the distal trachea.
D. Bronchoscopy shows a pedunculated vesicular mass in the distal trachea, which was confirmed to be fibrolipomatous hamartoma.
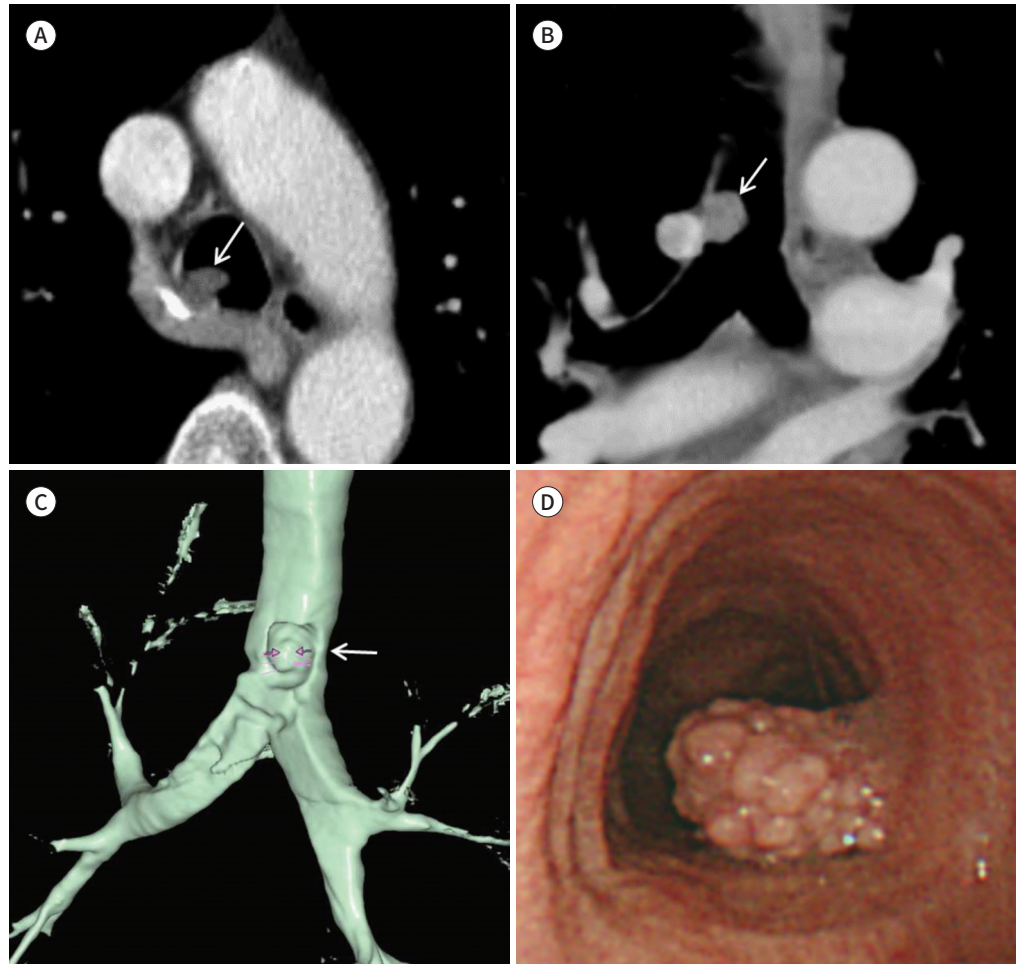
TUBERCULOSIS

Endobronchial involvement of tuberculosis (EBTB) occurs in approximately 2%–4% of patients with pulmonary tuberculosis. EBTB has been reported to be more common in females. Although the exact etiology is not well known, possible causes include a longer exposure to tubercle bacilli as female patients have less expectorated sputum containing bacilli due to sociocultural and aesthetic factors. Structural differences may also play a role as female bronchi are narrower than those of males, which may make females more susceptible to EBTB. EBTB usually occurs in the majority of patients in the second or third decade, with a second peak also described in old age. Primary bronchi, bilateral superior lobar bronchi, and right middle lobar bronchus are the commonly affected sites; however, EBTB may affect any part of the bronchial tree. Chest radiographs may be normal in about 10%−20% of patients with EBTB, and many chest radiographic findings are not specific for the diagnosis of EBTB (26, 27).

In recent years, high-resolution CT (HRCT) has been found to be superior to conventional chest radiography and standard CT in the localization of disease in the pulmonary lobule and the evaluation of pulmonary parenchymal disease due to its high-resolution power and mini-

Fig. 16. An 80-year-old female with tuberculosis complaining of wheezing and chronic cough.
A, B. Contrast-enhanced CT shows segmental enhancing wall thickening and luminal narrowing (arrows) in the left main bronchus.
C. CT in the lung window setting shows ill-defined clustered small centrilobular nodules, suggestive of parenchymal tuberculosis in the left upper lobe.
D. The three-dimensional volume-rendering image of the airway shows mild luminal narrowing (arrow) in the distal trachea and smooth tapering of the left main bronchus.
E. Bronchoscopy shows a stenotic lumen of the left main bronchus and an upper lobe orifice with caseating necrotic mucosa. The endobronchial lesion was confirmed to be tuberculosis.
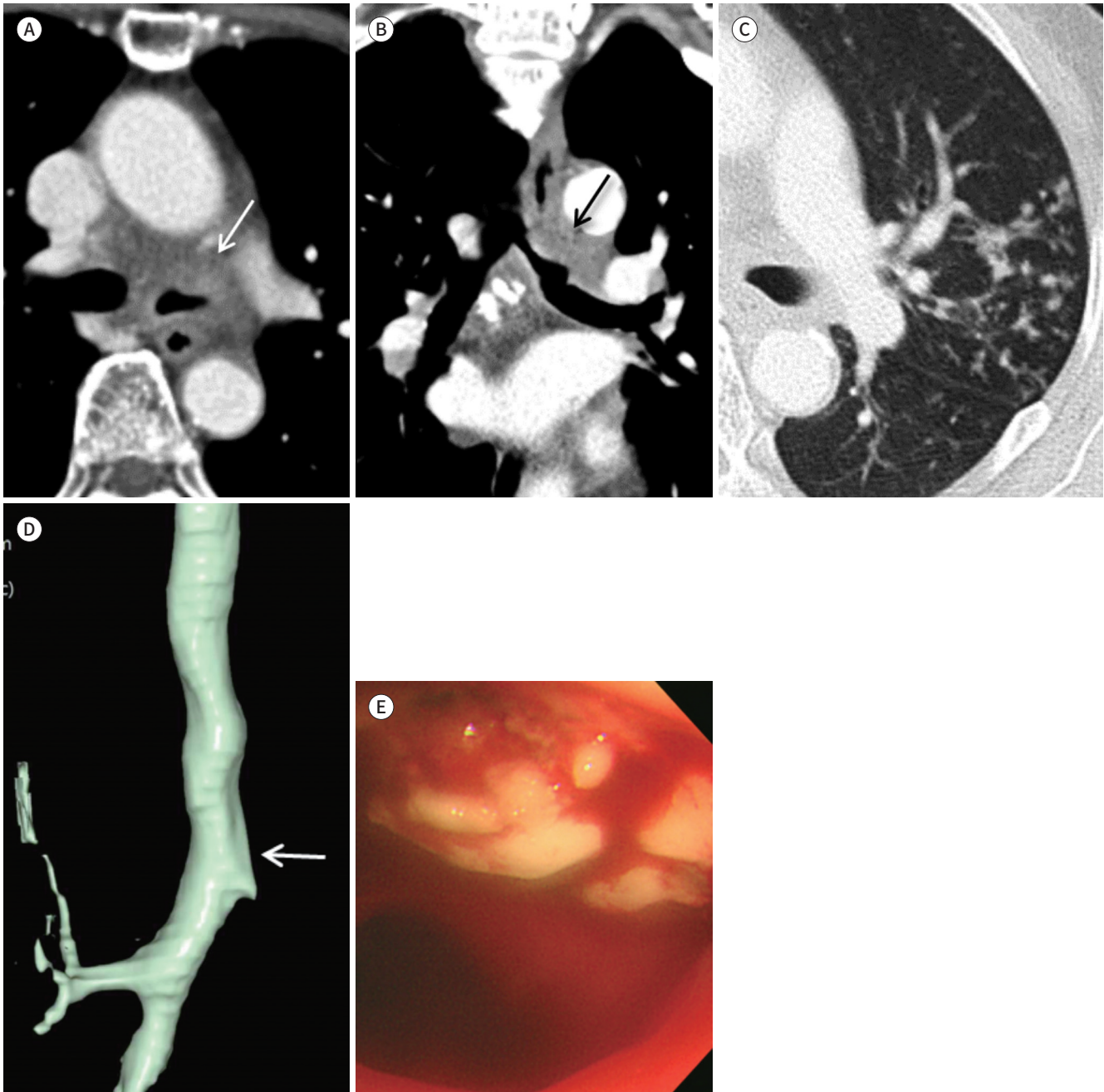
mal partial volume effect. Endobronchial involvement in pulmonary TB has been reported to be as high as 95% and 97% with HRCT scanning in various studies (26, 27).

CT findings include segmental bronchial narrowing with concentric wall thickening, complete endobronchial obstruction, extrinsic obstruction by adjacent lymph node enlargement, enlarging peribronchial soft tissue, and scarring (Fig. 16). Often, a neighboring caseous lymph node may erode the bronchial wall, which simulates a small intraluminal infiltrating nodule and is associated with a larger extraluminal component (iceberg tumor). Similarly, larger caseating erosions can compromise the bronchial lumen with the formation of large voluminous intraluminal masses. Alternatively, the granulation tissue and fibrosis associated with ulcerations can lead to narrowing of the lumen, which is more commonly observed in the left main bronchus. Even for patients with highly suspicious chest CT findings, bronchoscopy with a histopathological or microbiological confirmation is still required for a definite diagnosis of EBTB (26, 27).

FUNGUS

Fungal species that infect the trachea or bronchi include Aspergillus, Coccidioides, Candida, Cryptococcus, and Histoplasma organisms. Up to 80% of patients with a fungal infection of the tracheobronchial tree have an underlying condition that compromises the immune system. Depending on a patient's immunocompetence, Aspergillus infection may manifest as allergic bronchopulmonary aspergillosis (ABPA), intrabronchial aspergilloma, semi-invasive necrotizing bronchial aspergillosis, or invasive acute tracheobronchitis. ABPA is a hypersensitivity reaction to Aspergillus organisms in patients with a pre-existing pulmonary disease such as asthma or cystic fibrosis. Excessive mucus production and ciliary dysfunction lead to mucoid impaction without mucosal invasion. Chest radiography may not show airway abnormalities (1, 12). Invasive pulmonary aspergillosis is caused by Aspergillus species, particularly *Aspergillus fumigatus*, and involves normal lung tissue. It usually occurs in immunocompromised patients, especially in patients with neutropenia. Invasive pulmonary aspergillosis has been categorized as angioinvasive and an airway centered invasive form depending on where the Aspergillus mainly invades. Airway centered invasive aspergillosis accounts for 14%–34% of the cases of invasive aspergillosis in immunocompromised patients. In immunocompetent patients even without chronic underlying disease such as diabetes mellitus, airway centered invasive pulmonary aspergillosis occurs very rarely (28).

CT typically shows intraluminal nodules or masses of soft-tissue attenuation in the tracheobronchial tree, airway wall thickening, airway stenosis, and occasionally intramural air. Bronchiectasis or airway compression from lymphadenopathy may be present. In ABPA, fingerlike opacities of soft-tissue attenuation ("finger-in-glove") are a sign of mucoid impaction and bronchiectasis (Fig. 17) (1, 12). Typical diagnostic findings of the airway-centered invasive form are patchy peribronchial consolidation, small airway lesions, including centrilobular nodules, and bronchiectasis (Fig. 18) (28). Although imaging can be suggestive of airway mycosis, a definite diagnosis is typically made by fungal cultures obtained at bronchoscopy (1, 12).

Fig. 17. A 52-year-old female with allergic bronchopulmonary aspergillosis complaining of severe dyspnea. The patient had underlying bronchial asthma with elevated eosinophil levels.
A. Chest CT in the lung window setting shows diffuse wall thickening of the visible bronchi in the right lung (arrow).
B. Chest CT in the lung window setting shows mucus impaction in the left lingular segment (arrow) and bronchiectasis in the right lower lobe (arrowhead).
This figure has been adapted with permission from Dong-A University Hospital, Busan, South Korea.
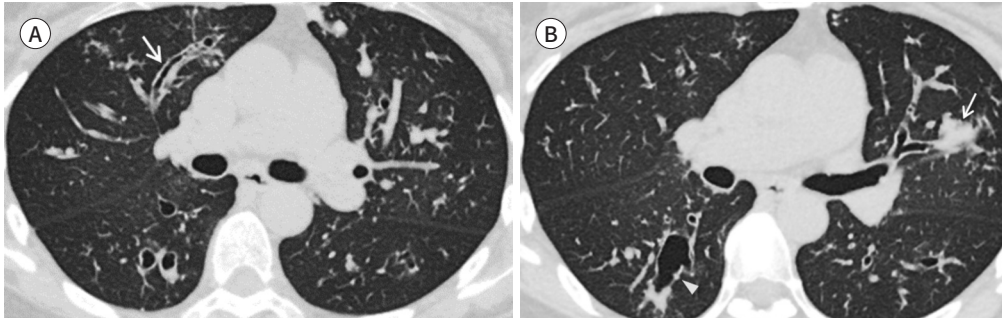

Fig. 18. A 62-year-old male with airway-invasive pulmonary aspergillosis complaining of persistent fever and cough for 3 weeks. The patient had underlying diabetes mellitus and hepatitis B.
A-C. Chest CT in the lung window setting shows diffuse wall thickening of the visible bronchi in both lungs (arrows) and ill-defined centrilobular nodules (arrowheads).
D. Bronchoscopy shows a white nodular lesion in the right upper lobar bronchus, which biopsy confirmed to be chronic active inflammation with a focal area of necrosis and fungal hyphae.
This figure has been adapted with permission from Inje University Busan Paik Hospital, Busan, South Korea.
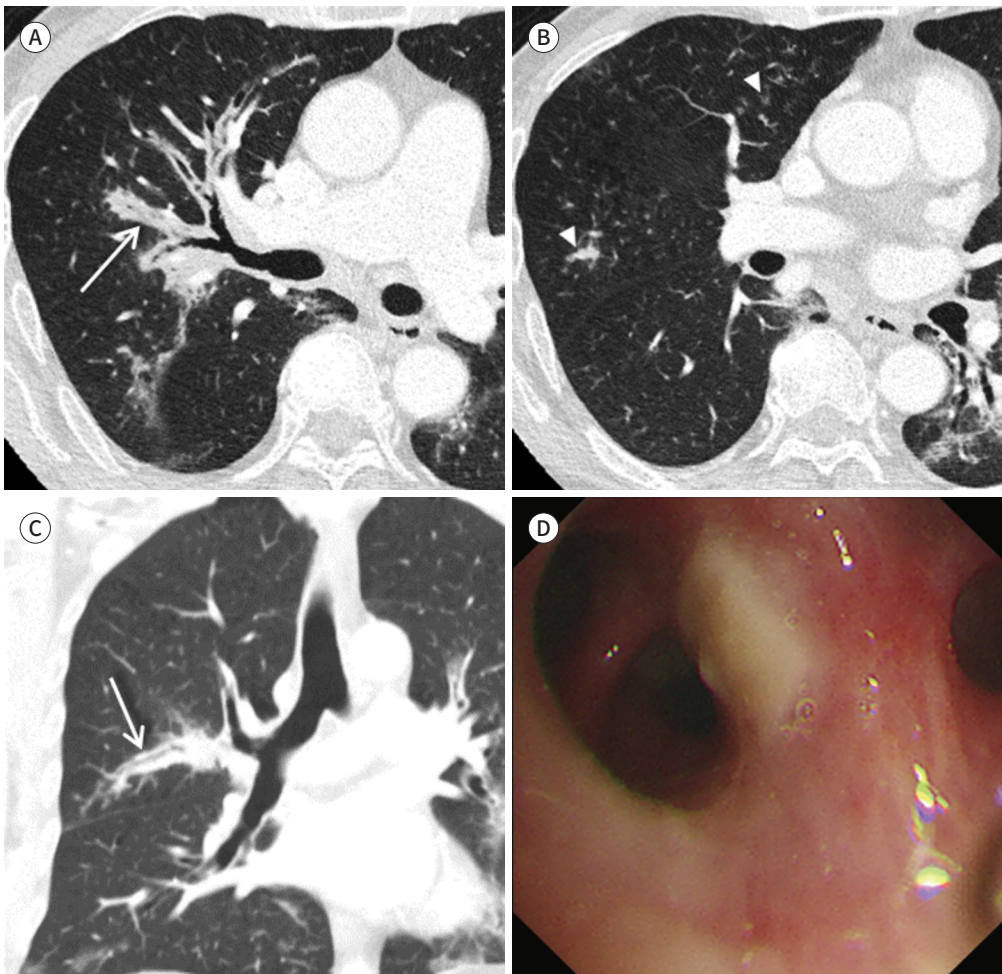
VIRAL AND OTHER PNEUMONIAS

Viruses are the most common causes of acute respiratory infections, and causative agents of lower respiratory tract infection vary according to patient age and immunity. Diffuse swelling associated with signs of upper airway obstruction is seen in the setting of childhood infections, such as with parainfluenza types 1–3, influenza A and B viruses, adenoviruses, coronavirus NL63, and respiratory syncytial virus. In adults, upper airway obstructive symptoms are unlikely due to the larger diameter of the adult trachea compared to that in children. Infectious processes in adults are associated with risk factors such as immunocompromised states or focal damage to the tracheal mucosa from etiologies such as intubation or tracheostomy. Overall, most of the cases of viral tracheitis result from parainfluenza or respiratory syncytial virus infection, which can lead to subglottic or laryngeal narrowing (29, 30).

CT findings of viral pneumonia are diverse and may be affected by the immune status of the host and the underlying pathophysiology of the viral pathogen. The viruses usually appear as multifocal patchy consolidation with ground glass opacity, and centrilobular nodules with bronchial wall thickening are also noticed (Fig. 19) (29, 30).

Fig. 19. A 79-year-old female with fever, cough, sputum, and dyspnea, who was confirmed with influenza A (H1N1) infection through a throat swab.
A-C. Chest CT shows diffuse mild wall thickening (arrows) of the trachea and both central bronchi visible.
D-F. Follow-up chest CT after Tamiflu® (oseltamivir phosphate) treatment shows a decreased interval change of diffuse bronchial wall thickening (arrows).
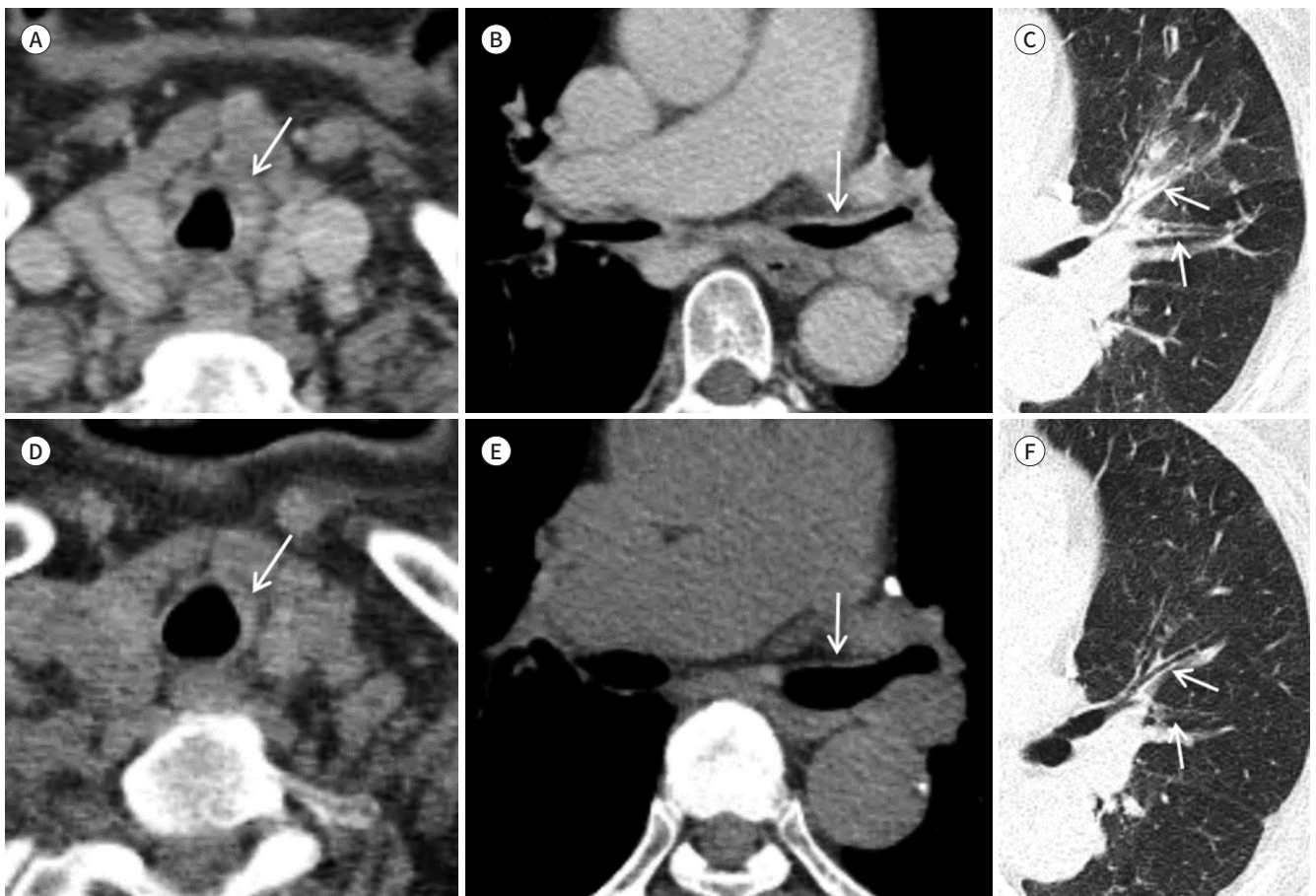
INFLAMMATION

ASTHMA

Asthma is an inflammatory disease of the lungs characterized by increased airway reactivity to various stimuli and by airflow obstruction that is at least partially reversible. Histologically, asthma is characterized by the presence of chronic inflammation of the airways mainly involving medium-sized and small bronchi. The bronchi are thickened by the combination of edema and increased amount of smooth muscle and size of the mucous glands. These histologic changes are found on HRCT by the presence of bronchial wall thickening and narrowing of the bronchial lumen. The prevalence of bronchial thickening on HRCT in patients with asthma reportedly ranges from 44% to 92%. Histologic bronchiolar abnormalities seen in asthma include bronchiolar wall thickening, mucus stasis in bronchioles, and constrictive bronchiolitis (31).

HRCT manifestations include thickening of the bronchial wall, narrowing of the bronchial lumen, areas of decreased attenuation and vascularity on inspiratory scans, and air trapping on expiratory scans (Fig. 20). Prominent centrilobular structures or small centrilobular opacities have been reported in 10%–20% of patients with asthma. Other findings that are seen with increased frequency in patients with asthma are bronchiectasis and emphysema (31).

VASCULITIS

Granulomatosis with polyangiitis (GPA), formerly known as Wegener's granulomatosis, is an idiopathic disease characterized by multisystemic necrotizing granulomatous vasculitis. There is no particular age predilection. Up to half of the patients with GPA have tracheobronchial tree involvement, which rarely is the only manifestation of the disease. Patients may present with respiratory signs and symptoms, and frequently have elevated serum c-antineutrophil antibodies against protease 3 in cytoplasmic granules (c-ANCA). In large airway GPA, acute inflammatory mucosal abnormalities range from edema to ulcers. These abnormalities commonly cause airway wall thickening and fixed or reversible stenosis, often of the upper trachea (1, 9, 12).

On CT, signs of large airway involvement include smooth or nodular circumferential thickening of the tracheobronchial wall that leads to a single stenosis or multiple stenoses (Fig. 21). Approximately 25% of patients have subglottic stenosis, and approximately 10% of patients will have bronchial stenosis. Irregular calcifications of the tracheal cartilage rings and bronchiectasis can occur. Severe airway obstruction may lead to atelectasis. Additional airway and pulmonary findings including parenchymal nodules, cavitary nodules, and pleural effusions can aid in diagnosis (1, 9, 12).

RELAPSING POLYCHONDRITIS

Relapsing polychondritis (RPC) is a rare autoimmune disorder that results in inflammation and destruction of cartilaginous structures throughout the body, including the laryngotracheobronchial tree. The airway is involved in approximately 50% of patients (9).

On CT imaging, RPC is characterized by thickening of the anterior and lateral walls of the trachea (Fig. 22). In addition, the thickened walls demonstrate increased attenuation. There

Fig. 20. A 37-year-old female with recently aggravating cough and dyspnea who was diagnosed with asthma in the past.

A, B. Chest CT in the lung window setting show diffuse wall thickening (arrows) of the visible bronchi of both lungs and some endobronchial nodularities (arrowhead) in the right middle and lower lobes.

C. Chest radiography shows hyperinflation and diffuse bronchial wall thickening (arrow) in the central portion of both lungs. The pulmonary function test initially showed a severe decrease in FEV_1, which was less than 40% of the predicted value.

D. Bronchial wall thickening is no longer visible (arrow) on follow-up chest radiography after corticosteroid treatment. Clinical improvements were observed, and FEV_1 increased to 84.8% of the predicted value.

FEV_1 = forced expiratory volume in 1 second
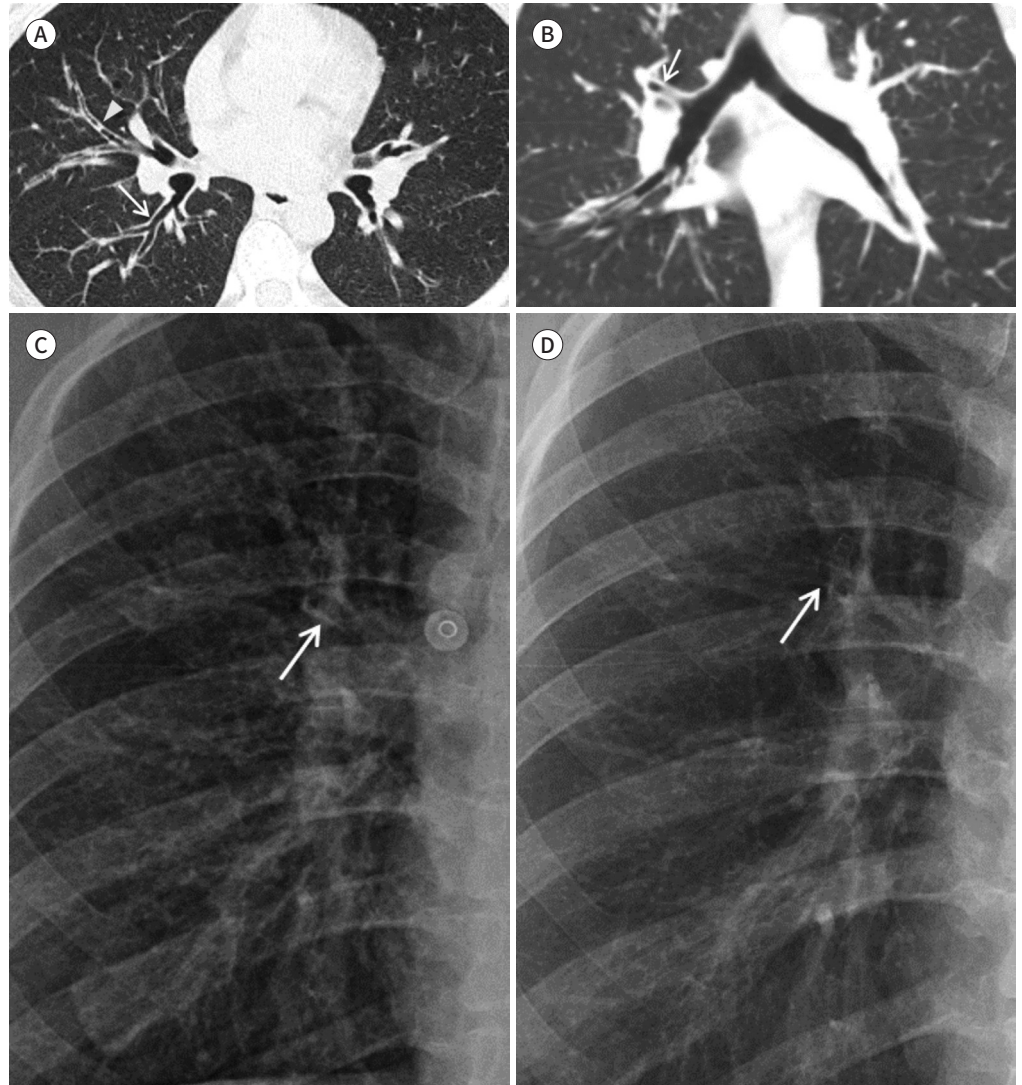
is often associated destruction of the cartilaginous tracheobronchial rings with sparing of the noncartilaginous posterior wall. Tracheomalacia and/or large airway stenosis may develop as sequelae (9).

Fig. 21. A 66-year-old male with GPA complaining of cough and sputum for 1 month.
A, B. Contrast-enhanced CT shows circumferential wall thickening of the trachea (arrows).
C, D. Contrast-enhanced CT shows cavitary and necrotic masses (arrows) in the lung parenchyma.
E-G. ^{18}F-FDG PET/CT images show increased fluorodeoxyglucose uptake in the trachea and parenchyma masses, which were confirmed with GPA by positive results using ANCA PR-3 antibody through surgical resection of the mass in the left upper lobe.
This figure has been adapted with permission from Pusan National University Hospital, Busan, South Korea.
ANCA = antineutrophil cytoplasmic antibody, GPA = granulomatosis with polyangiitis, ^{18}F-FDG = fluorine-18-fluorodeoxyglucose
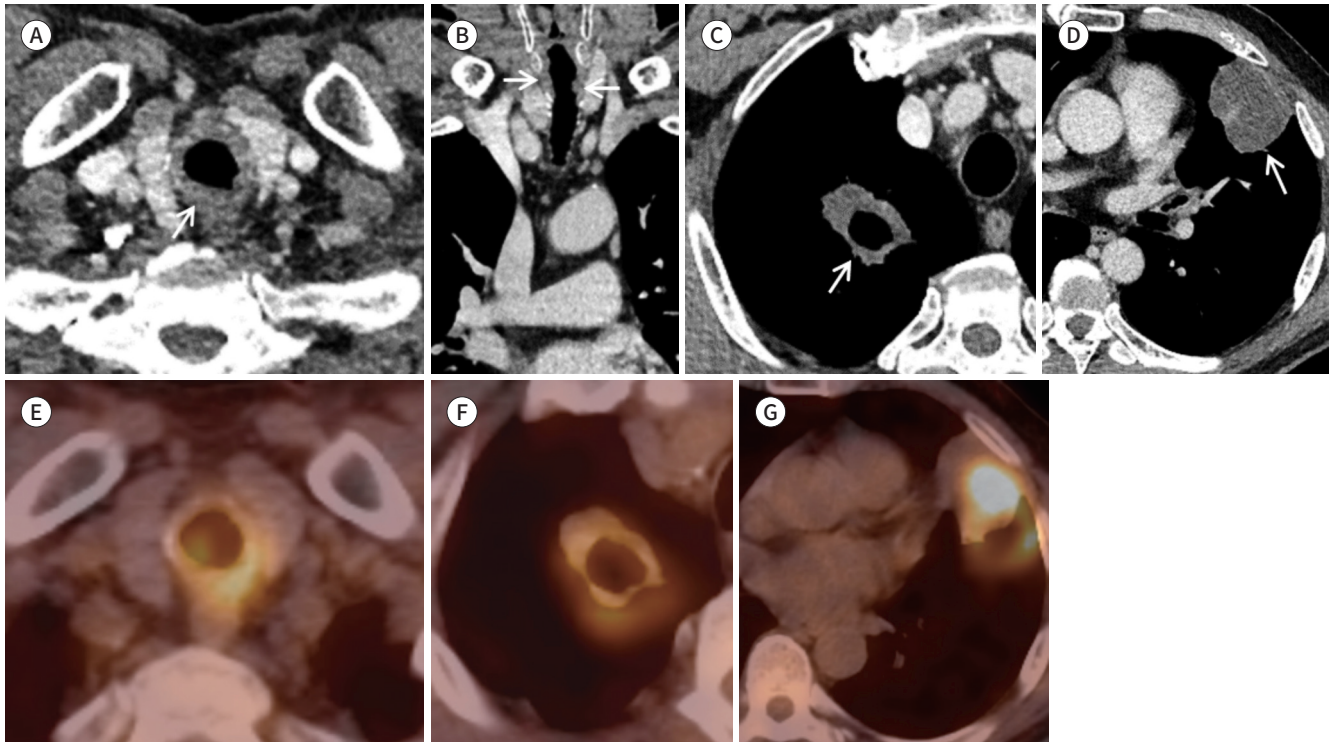
MISCELLANEOUS DISEASE

BRONCHIAL ANTHRACOFIBROSIS

   Bronchial anthracofibrosis (BAF) is a pulmonary disease caused by long-standing exposure to biomass fuel smoke. BAF is mostly seen in elderly female who have been exposed to dense smoke in poorly ventilated kitchens. The diagnostic criteria for BAF include: 1) long-standing history of biomass fuel smoke exposure, 2) multifocal bronchial narrowing on HRCT, 3) confirmed on bronchoscopy by visualization of bluish-black mucosal anthracotic pigmentation along with narrowing/distortion of the affected bronchus.

   On HCRT, multifocal bronchial narrowing is often considered to be the diagnosis hall mark of BAF and usually involves right middle and upper lobe bronchi (Fig. 23). BAF affects the segmental or lobar bronchi with sparing of trachea and the main bronchus in most of the patients. Peribronchial soft-tissue thickening or cuffing can raise suspicions of BAF. BAF can at times present with mediastinal lymphadenopathy and may develop calcification within the enlarged lymph nodes. These lymph nodes can cause extrinsic bronchial compression leading to lobar/segmental atelectasis. In addition, these can erode into the bronchus and subsequently lead to bronchostenosis (32).

Fig. 22. A 51-year-old female with relapsing polychondritis complaining of dyspnea for 5 months
A, B. Contrast-enhanced CT shows diffuse smooth wall thickening of the cartilaginous portion of the upper trachea (arrows).
C. The three-dimensional volume-rendering image of airway shows smooth luminal narrowing (arrows) in the upper trachea.
D, E. Laryngoscopy shows diffuse luminal narrowing of the trachea, particularly in the subglottic area. The patient had recurrent bilateral auricular chondritis, polyarthritis, and nasal chondritis with a saddle nose and was confirmed with relapsing polychondritis. The pulmonary function test showed a severe obstructive lung defect with a forced expiratory volume in 1 second of 54%.
E = esophagus
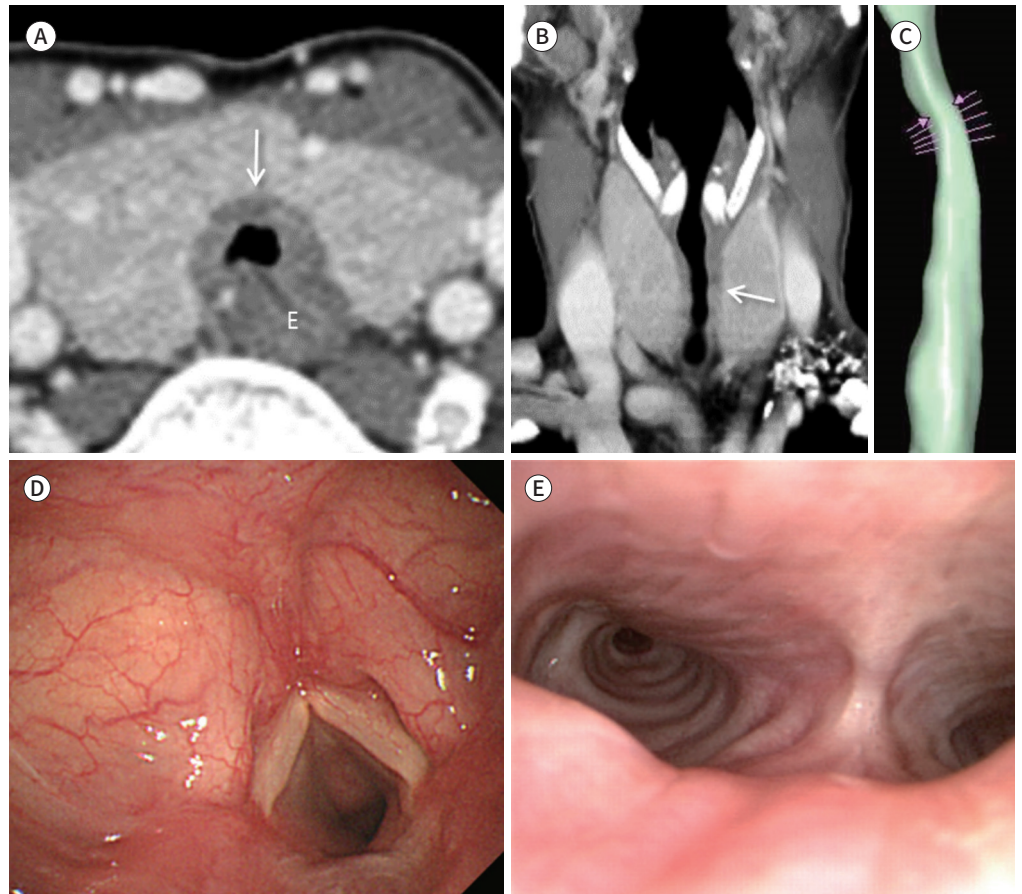
SARCOIDOSIS

Sarcoidosis is an idiopathic multisystemic disorder characterized by the formation of non-caseating granulomas. It typically involves the hilar and mediastinal lymph nodes and lung parenchyma. Tracheobronchial involvement is rare, affecting up to 3% of patients with sarcoidosis, and when present, most commonly involves the proximal trachea (9, 12).

CT imaging may demonstrate extrinsic compression of the airways by adjacent lymph nodes or primary infiltration of the tracheobronchial walls with noncaseating granulomas and the involvement of bronchi more commonly seen than the trachea (Fig. 24) (9, 12).

AMYLOIDOSIS

Amyloidosis is a rare disorder of unknown etiology characterized by the deposition of ab-

Fig. 23. A 65-year-old female confirmed with anthracofibrosis with cough and sputum for 5 months.
A. CT in the lung window setting shows diffuse bronchial wall thickening with luminal narrowing in the right upper lobe (arrows).
B, C. Contrast-enhanced CT shows symmetrically enlarged lymph nodes with calcification in the mediastinum and right hilar area (arrows).
D. Bronchoscopy shows a stenotic lumen of the right upper lobe orifice with swollen hyperemic mucosa, which was confirmed to be anthracofibrosis.
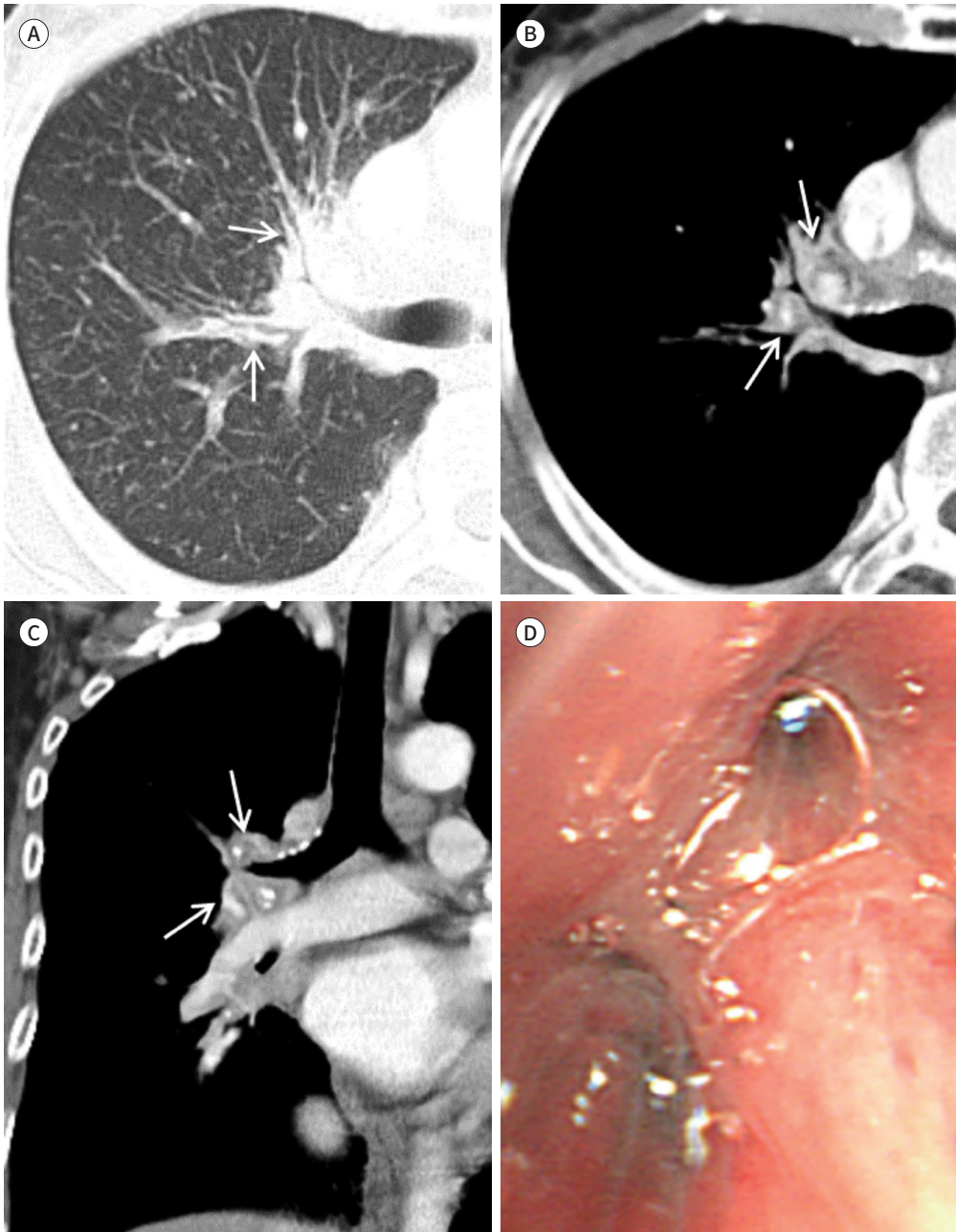
normal proteinaceous material in extracellular tissues and various organs throughout the body. Pulmonary amyloidosis can be found in three forms, diffuse interstitial deposits, pulmonary nodules, and submucosal tracheobronchial deposits. Involvement of the tracheobronchial tree, although rare, is the most common manifestation of thoracic amyloidosis (9, 12).

대한영상의학회지

Fig. 24. A 54-year-old female confirmed with sarcoidosis without respiratory symptoms.
A. CT in the lung window setting shows irregular bronchial wall thickening with small perilymphatic nodules (arrow) in the right upper lobe.
B. Contrast-enhanced CT shows symmetrically enlarged lymph nodes (arrows) in the mediastinum and both hilar areas.
C. Follow-up CT after corticosteroid treatment shows a decreased interval change of the bronchial wall thickening (arrow) and perilymphatic nodules.
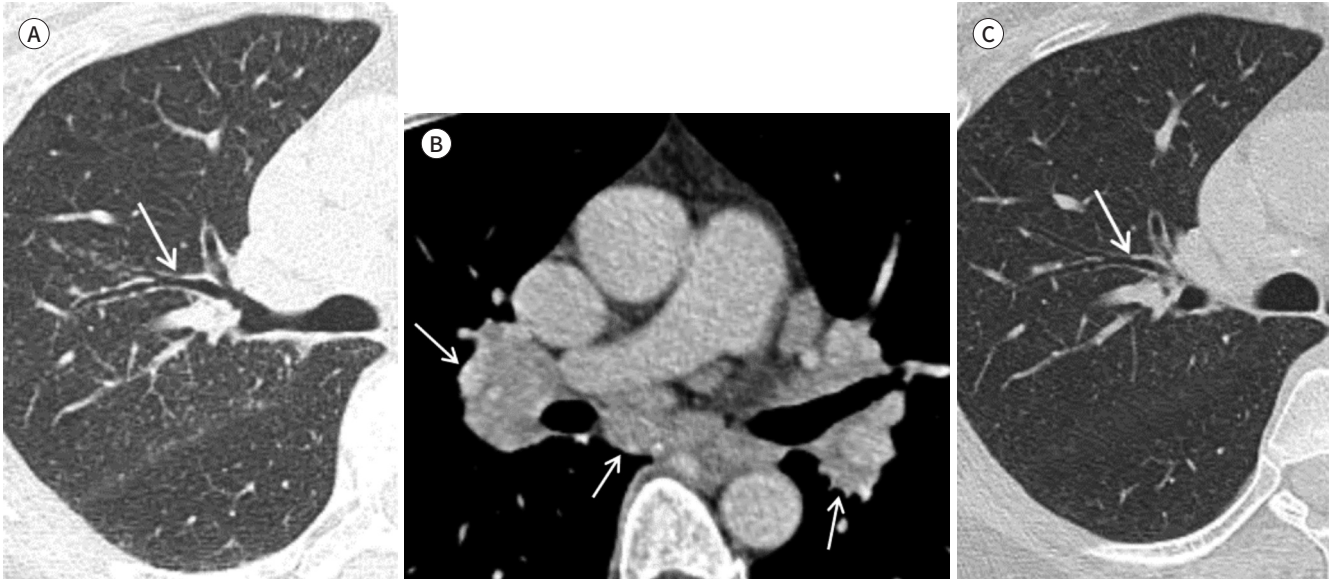
Fig. 25. A 75-year-old male confirmed with tracheobronchopathia osteochondroplastica without respiratory symptoms.
A, B. Contrast-enhanced CT shows irregular wall thickening with calcification in the cartilaginous portion of the trachea (arrows).
C. The three-dimensional volume-rendering image of the airway shows diffuse irregular luminal narrowing of the trachea.
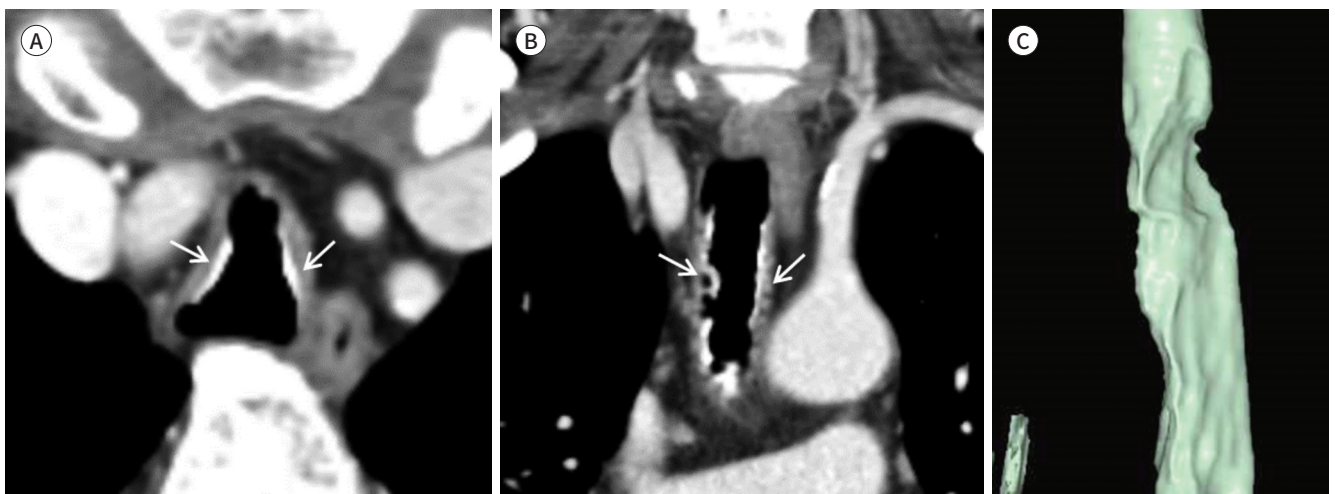
On CT, diffuse nodular thickening of the trachea and mainstem bronchi can be seen. Most frequently, the subglottic trachea is involved. The nodular areas will commonly calcify, and thus tracheobronchial amyloidosis may resemble tracheobronchopathia osteochondroplastica (TPO). However, in tracheobronchial amyloidosis, there is circumferential wall involvement whereas the posterior wall is spared in TPO. Bronchial occlusion or stenosis are known sequelae (9, 12).

TRACHEOBRONCHOPATHIA OSTEOCHONDROPLASTICA

TPO is characterized by submucosal osseous and cartilaginous deposits arising from tracheobronchial enchondromas anterolaterally, sparing the posterior membrane. It classically

Fig. 26. A 69-year-old male with IgG4-related pulmonary involvement complaining of 10 kg weight loss within the past 2 months and nocturnal fever.

A-D. Chest CT shows diffuse smooth bronchial wall thickening (arrows) and multiple ill-defined patchy or well-defined nodular lesions with mild enhancement (arrowheads).

E, F. Follow-up CT 2 months after corticosteroid treatment shows decreased interval changes in bronchial wall thickening and nodular lesions. His serum IgG/IgG4 ratio was 2227/4960, and IgG4 was positive in the nasal cavity biopsy specimen, confirming the diagnosis of IgG4-related disease.

Ig = immunoglobulin
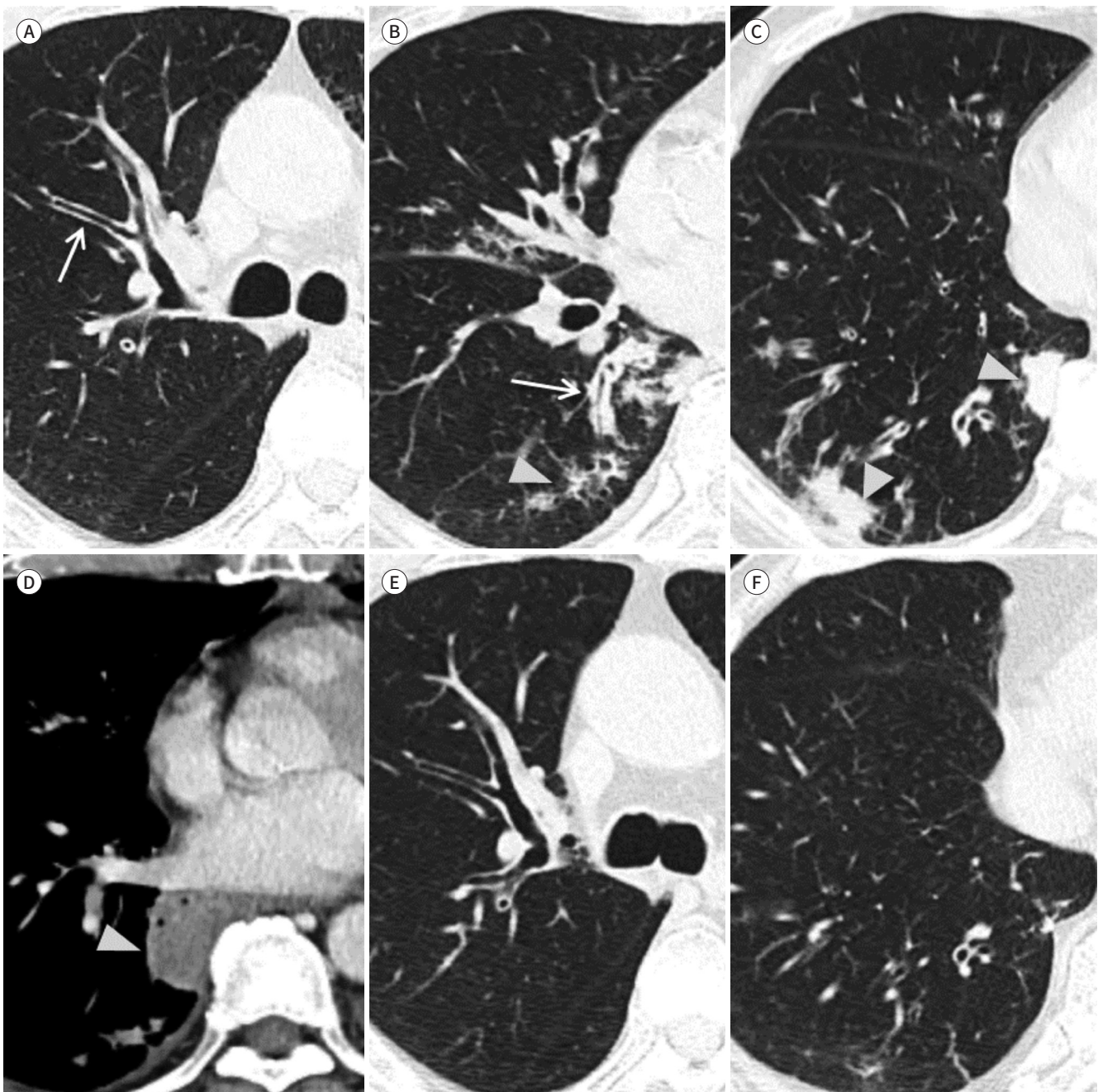
affects the lower two-thirds of the trachea, with or without the involvement of mainstem bronchi. TPO has a slight predilection for male, typically occurs in the sixth decade, and is usually an incidental finding on chest CT performed for other reasons. The patients are commonly asymptomatic but may present with hemoptysis, dyspnea, stridor, or hoarseness (9, 12).

On CT, TPO appears as 1–3-mm calcified nodules arising from the cartilaginous, anterior ring of the trachea. These calcified, nodular excrescences protrude into the lumen of the airway resulting in luminal narrowing (Fig. 25). The posterior wall of the trachea and mainstem bronchi is characteristically spared, which helps to distinguish this from other disease processes affecting the central airways (9, 12).

IGG4-RELATED PULMONARY INVOLVEMENT

Immunoglobulin (Ig) G4-related sclerosing disease (ISD) is a systemic fibroinflammatory disease associated with elevated circulating levels of IgG4. ISD has been described mainly in adults, more often in males (70%–80%) than females, with a median age of 60–65 years (range 17–80 years). The intrathoracic manifestations of ISD appear to be heterogeneous, involving not only the lung parenchyma but also the intrathoracic lymph nodes, mediastinum, and pleura, as well as the airways. There have been rare reports of airway disease associated with ISD that have exhibited central airway stenosis (33).

CT scanning shows intrathoracic lymphadenopathy and thickening of the bronchovascular bundle, resembling the features seen in sarcoidosis (Fig. 26). Another airway manifestation described with ISD is extrinsic compression of the central airways due to fibrosing mediastinitis and bronchiectasis. Bronchiectasis seen in this context appears to be associated with parenchymal fibrosis in the peripheral zones of the lung, i.e., traction bronchiectasis, rather than involvement of the proximal large airways (33).

OTHER CONDITIONS

ACQUIRED TRACHEOBRONCHOMALACIA (SENILE CHANGE)

Tracheobronchomalacia (TBM) is defined as collapse (greater than 50%–70%) of the tracheobronchial wall with expiration. It is characterized by an excessive expiratory airway collapse due to weakness of the airway walls secondary to alteration of the cartilaginous supports and/or redundancy of the posterior tracheal membranous wall. The most common type of the disease is the compromise of both the trachea and bronchi (63%), followed by isolated tracheal involvement (22%) and isolated bronchial involvement (15%). TBM may be idiopathic, associated with prematurity and congenital cartilaginous weakness among other congenital anomalies. The congenital form is usually self-limiting within the first 2 years of life. The acquired form is most commonly associated with prolonged mechanical endotracheal intubation, chronic airway inflammation including COPD, and RPC (1, 2, 12).

The traditional diagnosis is based on a bronchoscopic decrease in the tracheal diameter of more than 50% during expiration. MDCT is now considered a first-line screening tool for clinically suspected TBM and may also serve as an adjunct to bronchoscopy in preoperative planning and even as an alternative to bronchoscopy in pediatric or elderly populations. On an inspiratory MDCT scan, a lunate tracheal configuration (coronal to sagittal diameter ratio

> 1) is highly specific for TBM, but it has low sensitivity. On the dynamic MDCT scan, a crescentic pattern, also called the "frown sign", shows marked anterior bulging of the posterior membrane and is highly specific for TBM (Fig. 27) (1, 2, 12).

POSTINTUBATION TRACHEAL STENOSIS

Iatrogenic tracheal injury is a well-known complication of endotracheal intubation and tracheostomy. In postintubation patients, the most common site of stricture is at the level of the inflated cuff (upper thoracic trachea, usually around the second or third thoracic vertebral level). The stricture occurs when cuff pressures exceed capillary arterial pressure causing ischemia of the adjacent mucosa, leading to fibrotic narrowing, usually within 3–6 weeks after removal. Risk factors include prolonged intubation and intrinsic patient characteristics such

**Fig. 27.** An 83-year-old male with acquired tracheobronchomalacia complaining of dyspnea.
A, B. Inspiratory CT shows widening of the tracheal coronal diameter.
C. The airway analysis image shows the plane area of the trachea, which is calculated to be 289.8 mm².
D, E. Expiratory CT shows significant collapse of the airway lumen, including the trachea and both main bronchi.
F. The airway analysis image at the same level of C shows a decreased plane area of the trachea, which is 90.0 mm².
D_{in} = minimum inner diameter/maximum inner diameter, D_{out} = minimum outer diameter/maximum outer diameter, LA = plane area of the airway, WA = wall area, WA% = (WA[WA+LA]) × 100, WT = wall thickness, WT% = (WT/[mean diameter/2]) × 100
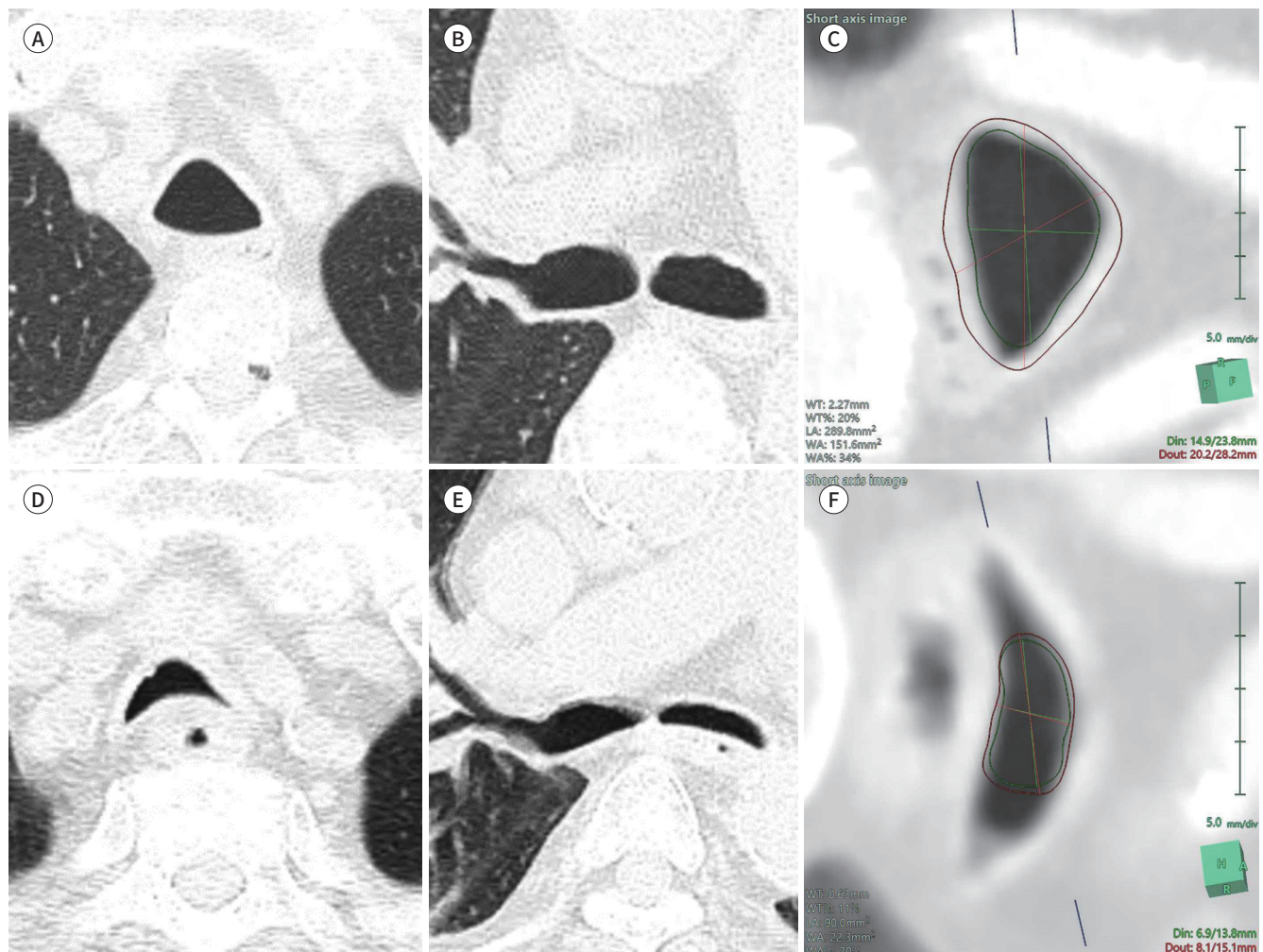
as female sex, smoking status, and a history of diabetes mellitus (9).

CT imaging demonstrates circumferential subglottic tracheal wall thickening leading to short segment narrowing in the region of the previously located cuff, usually 3 to 6 cm above the carina (Fig. 28). In posttracheostomy patients, the narrowing is most often located at the prior stoma site; however, the cuff site is commonly affected in this patient population as well (9).

CONCLUSION

A broad spectrum of pathologies can involve the tracheobronchial airway and patients are

Fig. 28. A 58-year-old female with postintubation tracheal stenosis complaining of dyspnea. The patient had undergone intubation 2 months before.
A, B. CT with contrast enhancement showing circumferential wall thickening and luminal narrowing of the upper trachea (arrows).
C. The three-dimensional volume-rendering image of the airway shows significant focal stenosis (arrows) of the upper trachea. The pulmonary function test showed a mild obstructive lung defect with an forced expiratory volume in 1 second of 79%.
D. CT at the time of intubation shows an expanded cuff and normal tracheal wall thickness at the same level as the current stenotic site.
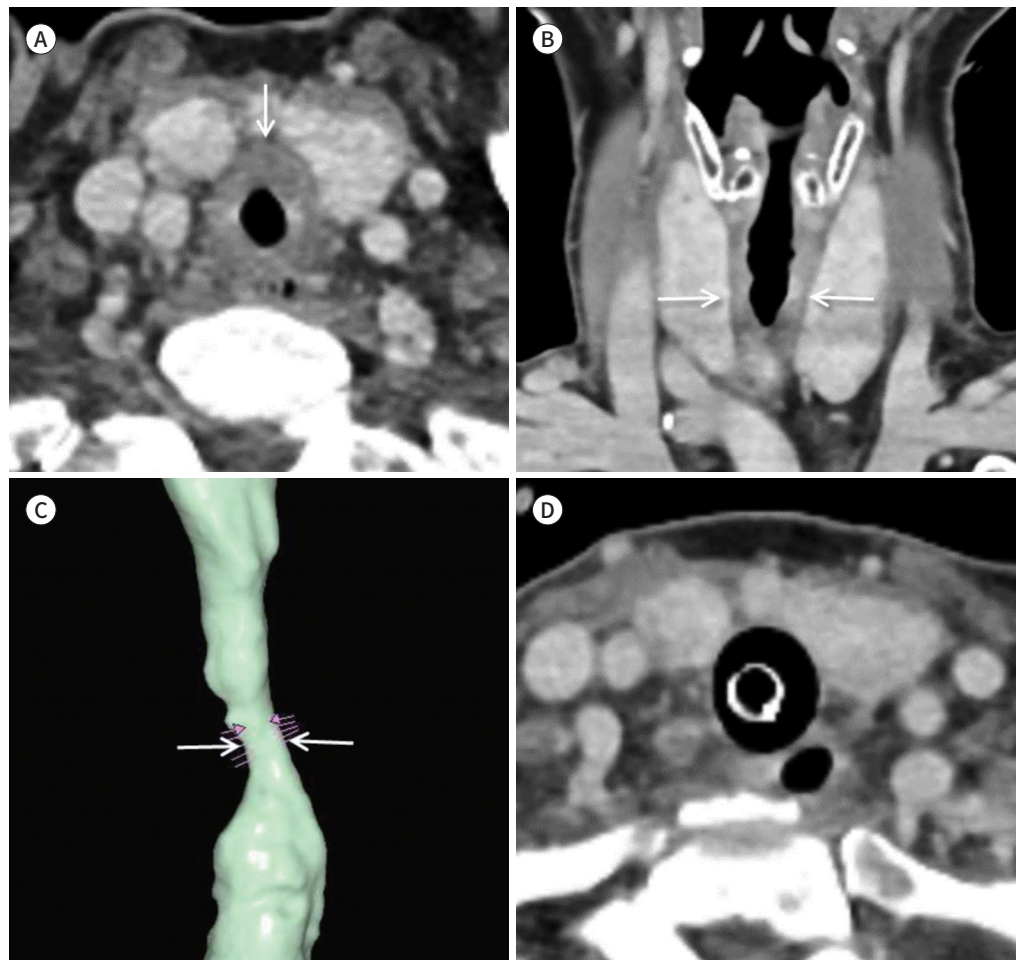
often initially misdiagnosed with more common diseases such as asthma or COPD as they exhibit similar clinical manifestations. Imaging plays a crucial role in evaluating these abnormalities and MDCT is the imaging test of choice. Analysis of characteristic features of the airways on MDCT images and even on post-processing tools will allow radiologists to detect tracheobronchial lesions, help narrow differential diagnosis, and assist physicians in finding lesions through bronchoscopy.

Supplementary Video Legend

Video 1. Virtual bronchoscopy pathway tracing image of peripheral lung cancer.

Supplementary Materials

The online-only Data Supplement is available with this article at http://dx.doi.org/10.3348/jksr.2020.0212.

Author Contributions

Conceptualization, K.H.; data curation, K.H.; project administration, K.H.; visualization, all authors; writing—original draft, all authors; and writing—review & editing, all authors.

Conflicts of Interest

The authors have no potential conflicts of interest to disclose.

Funding

None

REFERENCES

1. Heidinger BH, Occhipinti M, Eisenberg RL, Bankier AA. Imaging of large airways disorders. *AJR Am J Roentgenol* 2015;205:41-56
2. Barnes D, Gutiérrez Chacoff J, Benegas M, Perea RJ, de Caralt TM, Ramirez J, et al. Central airway pathology: clinic features, CT findings with pathologic and virtual endoscopy correlation. *Insights Imaging* 2017;8:255-270
3. Park CM, Goo JM, Lee HJ, Kim MA, Lee CH, Kang MJ. Tumors in the tracheobronchial tree: CT and FDG PET features. *Radiographics* 2009;29:55-71
4. Stevic R, Milenkovic B. Tracheobronchial tumors. *J Thorac Dis* 2016;8:3401-3413
5. Prince JS, Duhamel DR, Levin DL, Harrell JH, Friedman PJ. Nonneoplastic lesions of the tracheobronchial wall: radiologic findings with bronchoscopic correlation. *Radiographics* 2002;22 Spec No:S215-S230
6. Jugpal TS, Garg A, Sethi GR, Daga MK, Kumar J. Multi-detector computed tomography imaging of large airway pathology: a pictorial review. *World J Radiol* 2015;7:459-474
7. Al-Qadi MO, Artenstein AW, Braman SS. The "forgotten zone": acquired disorders of the trachea in adults. *Respir Med* 2013;107:1301-1313
8. Chung JH, Kanne JP, Gilman MD. CT of diffuse tracheal diseases. *AJR Am J Roentgenol* 2011;196:W240-W246
9. Lawrence DA, Branson B, Oliva I, Rubinowitz A. The wonderful world of the windpipe: a review of central airway anatomy and pathology. *Can Assoc Radiol J* 2015;66:30-43
10. Webb WR. Thin-section CT of the secondary pulmonary lobule: anatomy and the image--the 2004 Fleischner lecture. *Radiology* 2006;239:322-338
11. De Wever W, Vandecaveye V, Lanciotti S, Verschakelen JA. Multidetector CT-generated virtual bronchoscopy: an illustrated review of the potential clinical indications. *Eur Respir J* 2004;23:776-782
12. Sims SE, Li F, Lostracco T, Chaturvedi A, Son H, Wandtke J, et al. Multidimensional evaluation of tracheobronchial disease in adults. *Insights Imaging* 2016;7:431-448
13. Tirumani H, Rosenthal MH, Tirumani SH, Shinagare AB, Krajewski KM, Ramaiya NH. Esophageal carcinoma:

current concepts in the role of imaging in staging and management. *Can Assoc Radiol J* 2015;66:130-139

14. Carneiro A, Sousa P, Rocha D, Preto A. Imaging findings in esophageal carcinoma: diagnosis, follow-up and complications. Proceedings of the 21st European Congress of Radiology; 2009 Mar 6-10; Vienna, Austria: ECR; 2009

15. Zhang J, Fu C, Cui K, Ma X. Papillary thyroid carcinoma with tracheal invasion: a case report. *Medicine (Baltimore)* 2019;98:e17033

16. Wang JC, Takashima S, Takayama F, Kawakami S, Saito A, Matsushita T, et al. Tracheal invasion by thyroid carcinoma: prediction using MR imaging. *AJR Am J Roentgenol* 2001;177:929-936

17. Kiryu T, Hoshi H, Matsui E, Iwata H, Kokubo M, Shimokawa K, et al. Endotracheal/endobronchial metastases: clinicopathologic study with special reference to developmental modes. *Chest* 2001;119:768-775

18. Koletsis EN, Kalogeropoulou C, Prodromaki E, Kagadis GC, Katsanos K, Spiropoulos K, et al. Tumoral and non-tumoral trachea stenoses: evaluation with three-dimensional CT and virtual bronchoscopy. *J Cardiothorac Surg* 2007;2:18

19. Park CM, Goo JM, Choi HJ, Choi SH, Eo H, Im JG. Endobronchial metastasis from renal cell carcinoma: CT findings in four patients. *Eur J Radiol* 2004;51:155-159

20. Kim AW, Liptay MJ, Saclarides TJ, Warren WH. Endobronchial colorectal metastasis versus primary lung cancer: a tale of two sleeve right upper lobectomies. *Interact Cardiovasc Thorac Surg* 2009;9:379-381

21. Fournel C, Bertoletti L, Nguyen B, Vergnon JM. Endobronchial metastases from colorectal cancers: natural history and role of interventional bronchoscopy. *Respiration* 2009;77:63-69

22. Chong S, Kim TS, Han J. Tracheal metastasis of lung cancer: CT findings in six patients. *AJR Am J Roentgenol* 2006;186:220-224

23. Yokoba M, Nishii Y, Hagiri S, Tanimura S, Honma K. Endobronchial metastasis from slow-growing lung cancer: a rare case report and review of the literature. *Respir Med CME* 2008;1:107-110

24. Kim EY, Kim TS, Choi JY, Han J, Kim H. Multiple tracheal metastases of lung cancer: CT and integrated PET/CT findings. *Clin Radiol* 2010;65:493-495

25. Ko JM, Jung JI, Park SH, Lee KY, Chung MH, Ahn MI, et al. Benign tumors of the tracheobronchial tree: CT-pathologic correlation. *AJR Am J Roentgenol* 2006;186:1304-1313

26. Das KM, Lababidi H, Al Dandan S, Raja S, Sakkijha H, Al Zoum M, et al. Computed tomography virtual bronchoscopy: normal variants, pitfalls, and spectrum of common and rare pathology. *Can Assoc Radiol J* 2015; 66:58-70

27. Shahzad T, Irfan M. Endobronchial tuberculosis-a review. *J Thorac Dis* 2016;8:3797-3802

28. Kim JH, Lee HL, Kim L, Kim JS, Kim YJ, Lee HY, et al. Airway centered invasive pulmonary aspergillosis in an immunocompetent patient: case report and literature review. *J Thorac Dis* 2016;8:E250-E254

29. Bedayat A, Yang E, Ghandili S, Galera P, Chalian H, Ansari-Gilani K, et al. Tracheobronchial tumors: radiologic-pathologic correlation of tumors and mimics. *Curr Probl Diagn Radiol* 2020;49:275-284

30. Koo HJ, Lim S, Choe J, Choi SH, Sung H, Do KH. Radiographic and CT features of viral pneumonia. *Radiographics* 2018;38:719-739

31. Silva CI, Colby TV, Müller NL. Asthma and associated conditions: high-resolution CT and pathologic findings. *AJR Am J Roentgenol* 2004;183:817-824

32. Shah A, Kunal S, Gothi R. Bronchial anthracofibrosis: the spectrum of radiological appearances. *Indian J Radiol Imaging* 2018;28:333-341

33. Ryu JH, Sekiguchi H, Yi ES. Pulmonary manifestations of immunoglobulin G4-related sclerosing disease. *Eur Respir J* 2012;39:180-186

협착을 유발하는 중심 기관지 병변들의 전산화단층촬영 소견 -시각화 및 정량화: 임상화보

최명진 · 강 희*

기관-기관지분지는 폐와 전신에 산소 공급을 위한 공기의 통로이며, 다양한 병적 상태들이 이러한 해부학적 부위를 침범할 수 있다. 다중 검출 전산화단층촬영은 다양한 기도 질환들의 진단을 위한 발견 및 특성화에 있어 중요한 역할을 한다. 가상 기관지경 검사나 자동 폐분석과 같은 후처리를 통해 영상 영상검사의 활용이 더욱 높아질 수 있다. 본 임상 화보에서는 벽 비후와 기관 내 결절의 형태로 나타나는 다양한 기관지 병변들의 다중 검출 전산화단층촬영에서의 소견 및 고차원적 영상 시각화와 분석 영상을 제공하고자 한다.

고신대학교 의과대학 고신대학교 복음병원 영상의학과